

Inelastic Collisions and Chemical Reactions of Molecules at Ultracold Temperatures

Goulven Quéméner, Naduvalath Balakrishnan

Department of Chemistry, University of Nevada Las Vegas, Las Vegas, NV 89154, USA

Alexander Dalgarno

ITAMP, Harvard-Smithsonian Center for Astrophysics, Cambridge, MA 02138, USA

(Dated: October 23, 2018)

Contents

I. Introduction	1
II. Inelastic atom - molecule collisions	2
A. Vibrational and rotational relaxation	2
1. Collisions at cold and ultracold temperatures	2
2. Shape resonances in molecular collisions	6
3. Feshbach resonances in molecular collisions	6
B. Quasi-resonant transitions	7
C. Atom - molecular ion collisions	8
III. Chemical Reactions at ultracold temperatures	9
A. Tunneling dominated reactions	9
1. Reactions at zero temperature	10
2. Feshbach resonances in reactive scattering	12
B. Barrierless reactions	14
1. Collision systems of three alkali metal atoms	14
2. Role of PES in determining ultracold reactions	16
3. Relaxation of vibrationally excited alkali metal dimers	18
4. Reactions of heteronuclear and isotopically substituted alkali-metal dimer systems	19
IV. Inelastic molecule - molecule collisions	20
A. Molecules in the ground vibrational state	20
B. Vibrationally inelastic transitions	22
V. Summary and outlook	24
References	24

I. INTRODUCTION

The development of techniques for cooling and trapping of a wide variety of atomic and molecular species in recent years has created exciting opportunities for probing and controlling atomic and molecular encounters with unprecedented precision [1]. While many of the initial studies of cold atoms and molecules were centered on the creation of dense samples of cold and ultracold matter, more recent work has focused on the manipulation and control of intermolecular interactions,

with the ultimate aim of achieving quantum control of atomic and molecular collisions [2]. Though the ideas of quantum control of chemical reactions were proposed many years ago, the ability to create ultracold molecules in specific quantum states has given further stimulus to this field. Its development requires that molecular properties and collisional behavior be well understood at cold and ultracold temperatures where the dynamics of molecules are dramatically different compared to collisions at elevated temperatures. Over the last ten years significant progress has been achieved both in theoretical and experimental works. The experimental methods such as photoassociation spectroscopy, magnetic tuning of Feshbach resonances, buffer-gas cooling, and Stark deceleration [3–6] have been developed and applied to a variety of molecular systems. Novel methods to study ultracold chemical reactions involving ion - molecule systems in a linear Paul trap have been proposed [7]. External control of chemical reactions using electric and magnetic fields is another area of active interest [8]. The aim of this chapter is to provide an overview of recent progress in characterizing molecular processes and chemical reactions at cold and ultracold temperatures with particular emphasis on theoretical developments in quantum dynamics simulations of atom - molecule collision systems over the last ten years.

In contrast to scattering at thermal energies, ultracold collisions offer fascinating and unique opportunities to study molecular encounters in the extreme quantum regime where the entire collision can be dominated by a single partial wave. One of the main motivations of current experimental efforts to create dense samples of ultracold molecules is to study the possibility of chemical reactions at temperatures close to absolute zero. While Wigner's law [9, 10] predicts that rate coefficients of exothermic processes are finite in the zero-energy limit it does not say if the rate coefficient will be large enough for reactions to be observable in an experiment. Nor does it say anything about how the rate coefficients at zero temperature depend on the interaction potential. Most chemical reactions between neutral atoms and molecules involve an energy barrier and it is not clear if chemical reactions between them generally occur with measurable rates at ultracold temperatures. Calculations for the $F + H_2$ reaction which proceeds by tunneling at low energies have shown that the reaction may occur with a significant rate at ultracold temperatures [11]. There is

also experimental and theoretical evidence that chemical reactions involving heavy-atom tunneling of carbon [12] and fluorine [13] atoms can occur with significant rate coefficients at low temperatures.

Photoassociation experiments involving alkali-metal systems have stimulated considerable interest in chemical reactivity in alkali-metal dimer - alkali-metal atom collisions at ultracold temperatures [14]. Rearrangement collisions in identical particle alkali-metal trimer systems occur without energy barrier and recent studies have demonstrated that chemical reactions in alkali-metal atom - alkali-metal dimer collisions may be very fast at ultracold temperatures. Unlike tunneling-dominated reactions, the limiting values of the rate coefficients for alkali-metal systems are less sensitive to vibrational excitation of the dimer.

In this chapter we give an overview of recent studies of ultracold atom - molecule collisions focusing on non-reactive and reactive systems and the effect of vibrational excitation of the molecule on the collisional outcome. We will discuss both tunneling-dominated and barrierless reactions and examine recent efforts in extending these studies to ionic systems as well as molecule - molecule systems. We consider mostly the novel aspects of collisional dynamics of atom - diatom systems at cold and ultracold temperatures with illustrative results for specific systems. For more comprehensive discussion of cold and ultracold collisions including reactive and non-reactive processes and the effect of external fields we refer the reader to several review articles [6, 8, 13–15] that have appeared in the last few years. For details of the theoretical formalisms we refer to the chapters by Hutson and by Tscherebul and Krems.

II. INELASTIC ATOM - MOLECULE COLLISIONS

Theoretical studies of ultracold molecules received intense interest after the success of ultracold atom photoassociation and buffer gas cooling experiments which demonstrated that a wide array of molecular systems with thermal and non-thermal vibrational energy distributions can be created in ultracold traps. The collisional loss of trapped molecules is an important issue in these experiments. Photoassociation produces molecules in highly excited vibrational levels. Whether the excited molecules decay by vibrational quenching or through chemical reaction is an intriguing question. While an extensive literature exists on the collisional relaxation of vibrationally excited molecules at elevated temperatures not much was known on the magnitude of the relaxation rate coefficients at temperatures lower than one Kelvin. Though a few earlier reports [16–18] on atom - diatom collisions in the Wigner threshold regime had been published, a detailed investigation of the depen-

dence of the relaxation rate coefficients on the internal energy of molecules and their sensitivity to details of the interaction potential has not been carried out. Here, we give a brief account of recent quantum dynamics calculations of vibrational and rotational energy transfer in atom - diatom collisions at cold and ultracold temperatures. We focus on a few representative systems to illustrate the main features of energy transfer in non-reactive atom - molecule collisions at ultracold temperatures and we show how the corresponding rate coefficients are influenced by rotational or vibrational excitation of the molecule.

A. Vibrational and rotational relaxation

1. Collisions at cold and ultracold temperatures

As discussed in the chapter by Hutson, at very low energies, scattering is dominated by s-waves and the scattering cross section can be expressed in terms of a single parameter called the scattering length. For single-channel scattering where only elastic scattering is possible, the scattering length is a real quantity and the magnitude of the cross section in the s-wave limit is given by $\sigma = 4\pi a^2$ where a is the scattering length. For multichannel scattering, as in vibrationally or rotationally inelastic collisions of molecules, the scattering length is a complex number and it is denoted as $a_{vj} = \alpha_{vj} - i\beta_{vj}$ where v and j are, respectively, the initial vibrational and rotational quantum numbers of the molecule [10, 19]. The limiting value of the elastic cross section in the presence of inelastic scattering is given by $\sigma_{vj}^{el} = 4\pi|a_{vj}|^2 = 4\pi(\alpha_{vj}^2 + \beta_{vj}^2)$. The total inelastic quenching cross section from a given initial rovibrational level of the molecule is related to the imaginary part of the scattering length through the relation $\sigma_{vj}^{in} = 4\pi\beta_{vj}/k_{vj}$ where k_{vj} is the wave vector in the incident channel. The quenching rate coefficient becomes constant at ultralow temperatures and is given by $k_{vj}^{in} = 4\pi\hbar\beta_{vj}/\mu$ at zero temperature where μ is the reduced mass of the collisional system. Thus, the rovibrational relaxation rate coefficients attain finite values for different initial vibrational and rotational levels of the molecule. The dependence of the rate coefficients on v and j has been an important issue in cold molecule research because exothermic vibrational and rotational relaxation collisions are a major pathway for trap loss in cooling and trapping experiments.

Initial studies of rotational and vibrational relaxation of atom - molecule systems at cold and ultracold temperatures have mostly focused on van der Waals systems such as He-H₂ [19–22], He-CO [23, 24], and He-O₂ [25]. Owing to the importance of some of these systems in astrophysical environments, extensive calculations of low-temperature behavior of rate coefficients have been performed for collisions of H₂ [19] and CO [23, 24] with

both ^3He and ^4He . For both systems reasonably accurate intermolecular potentials have been reported. The initial calculations on the $\text{He}-\text{H}_2$ system employed the potential energy surface (PES) of Muchnick and Russek (MR) [26]. For $\text{He}-\text{H}_2$ vibrational excitation of the H_2 molecule has a dramatic effect on the zero-temperature quenching rate coefficients. As illustrated in Fig. 1, the vibrational quenching rate coefficients increase by about three orders of magnitude between $v = 1$ and $v = 10$ of the H_2 molecule [19].

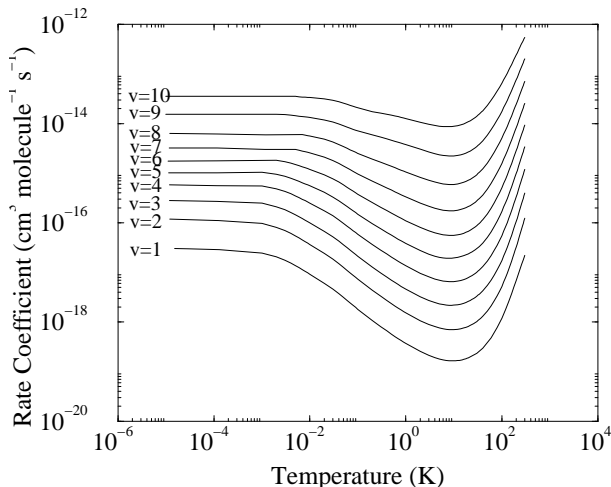


FIG. 1: Rate coefficients for the quenching of $\text{H}_2(v, j = 0)$ by collisions with He atoms as functions of the temperature for $v = 1 - 10$ of the H_2 molecule. Reproduced with permission from Balakrishnan et al. [19].

The quenching rate coefficients exhibit a minimum at around 10 K which roughly corresponds to the depth of the van der Waals interaction potential. This behavior appears to be a characteristic of vibrational quenching rate coefficients. For incident energies lower than the well depth the rate coefficient exhibits a minimum and with subsequent decrease in temperature the rate coefficient begins to increase before attaining the Wigner limit. For systems with deeper van der Waals wells the minimum is shifted to higher temperatures. Measurements of vibrational relaxation rate coefficients for the H_2-CO system have confirmed this behavior [27].

Balakrishnan, Forrey, and Dalgarno [28] also investigated vibrational relaxation of H_2 in collisions with H atoms for vibrational quantum numbers $v = 1 - 12$ of the H_2 molecule. They adopted a non-reactive scattering formalism and neglected the rotational motion of the H_2 molecule. The calculations showed that vibrational relaxation rate coefficients are strongly dependent on the initial vibrational level of the H_2 molecule. The relaxation rate coefficients were found to increase by about seven orders of magnitude between vibrational levels $v = 1$ and $v = 12$. The dramatic variation in the rate coefficients with increase in vibrational excitation was explained in terms of the matrix elements of the

interaction potential between the vibrational wavefunctions as functions of the atom - molecule center-of-mass separation.

Vibrational relaxation rate coefficients in atom - molecule systems are often influenced by van der Waals complexes formed during the collision process. Decay of these complexes leads to resonances in the energy dependence of the relaxation cross sections (see Fig. 2 for $\text{Ar}-\text{D}_2$ collisions). Applying effective range theory to describe ultracold collisions of the $\text{He}-\text{H}_2$ system, Balakrishnan et al. [19] and Forrey et al. [20] demonstrated that vibrational pre-dissociation lifetimes of resonances that lie close to the energy threshold can be derived accurately from the value of the zero-temperature quenching rate coefficient. This formalism was extended to describe vibrational relaxation of trapped molecules and it was shown that the vibrational relaxation rate is controlled by the most weakly bound state of the van der Waals complex [22]. In a related work Dashevskaya et al. [29] have shown that vibrational quenching of $\text{H}_2(v = 1, j = 0)$ at low temperatures can be described using a two channel approximation within the quasi-classical method provided appropriate parameters are employed in the calculations. Subsequently, Côté et al. [30] generalized this method to predict vibrational relaxation lifetimes of atom - diatom van der Waals complexes with energies near the dissociation threshold.

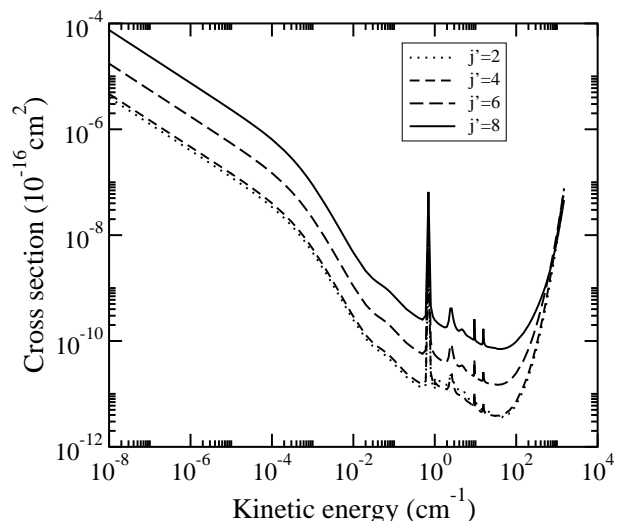


FIG. 2: Cross sections for quenching of the $v = 1, j = 0$ level of D_2 in collisions with Ar atoms resolved into the different rotational levels j' in $v' = 0$ as functions of the incident kinetic energy. Reproduced with permission from Uudus et al. [31].

Unlike in thermal energy collisions, the presence of a weakly bound state in the vicinity of a channel threshold can dramatically influence the cross sections in the ultracold regime. This is illustrated in Fig. 2 where the cross sections for vibrational relaxation of

$D_2(v = 1, j = 0)$ in collisions with Ar atoms [31] are presented over an energy range of $10^{-8} - 10^3 \text{ cm}^{-1}$. The cross sections exhibit a curvature characteristic of a resonant enhancement in the energy range $10^{-5} - 10^{-3} \text{ cm}^{-1}$. Such enhancement of the cross section can occur when the interaction potential supports a virtual state or a very weakly bound state near the channel threshold leading to a zero-energy resonance. The virtual state is characterized by a large negative scattering length while the bound state is characterized by a large positive scattering length. For the present case the real part of the scattering length is large and positive ($\alpha_{10} = 97.0 \text{ \AA}$) and the resonance occurs from the decay of a loosely bound van der Waals complex supported by the entrance channel potential. For energies below 10^{-2} cm^{-1} the cross section is dominated by s-wave scattering in the incident channel and the zero-energy resonance arises from s-wave scattering in the entrance channel.

The resonant enhancement is more clearly seen in the plot of the reaction probability as a function of the kinetic energy shown in Fig. 3. The probability peaks at an energy of $6.0 \times 10^{-4} \text{ cm}^{-1}$ which roughly corresponds to the binding energy of the quasibound state. The resonance appears in the scattering calculations at energies above the threshold due to its close proximity to the channel threshold. The binding energy of the quasibound state can be estimated using the scattering length approximation [10, 31]. The magnitude of the binding energy is given by $|E_b| = \hbar^2 \cos 2\gamma_{10} / (2\mu |a_{10}|^2)$ where μ is the reduced mass of the Ar- D_2 system, $a_{10} = \alpha_{10} - i\beta_{10}$ is the scattering length for the $v = 1, j = 0$ level, and $\gamma_{10} = \tan^{-1}(\beta_{10}/\alpha_{10})$. This yields a value of $|E_b| = 4.9 \times 10^{-4} \text{ cm}^{-1}$, in reasonable agreement with the exact value derived from scattering calculations.

A more accurate value of the binding energy can be obtained using the effective range formula given by Forrey et al. [20]:

$$|E_b| = \frac{\hbar^2}{\mu r_0^2} \left(1 - \frac{\alpha_{10} r_0}{|a_{10}|^2} - \sqrt{1 - \frac{2\alpha_{10} r_0}{|a_{10}|^2}} \right)$$

where r_0 is the effective range of the potential which may be evaluated by fitting the low energy behavior of the phase shift for the elastic channel to the standard effective range formula, $k_{10} \cot \delta_{10} = -1/\alpha_{10} + r_0 k_{10}^2/2$. For Ar- $D_2(v = 1, j = 0)$ collisions, the effective range formula yields $r_0 = 16.32 \text{ \AA}$. The resonance position calculated using the effective range approximation is $|E_b| = 5.95 \times 10^{-4} \text{ cm}^{-1}$, in excellent agreement with the value of $6.0 \times 10^{-4} \text{ cm}^{-1}$ obtained from the scattering calculations. It is generally very difficult to accurately evaluate energies of such weakly bound states using standard bound state codes and the effective range formula provides a convenient and reliable method to calculate binding energies of weakly bound states that lead to zero-energy resonances.

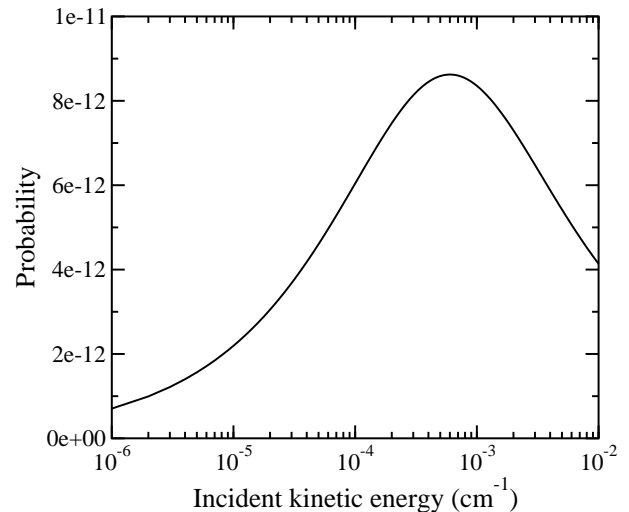


FIG. 3: Total probability of quenching of the $v = 1, j = 0$ level of D_2 in collisions with Ar atoms as a function of the incident kinetic energy. The peak value of the probability corresponds to a zero energy resonance. Reproduced with permission from Uudus et al. [31].

One of the challenging aspects of cold and ultracold collisions is the sensitivity to details of the interaction potential. Even the best available methods for the electronic structure calculations of PESs result in errors much larger than the collision energies in the cold and ultracold regime and the dynamics calculations are often sensitive to small changes in the interaction potential. To explore the sensitivity of cold and ultracold collisions to details of the interaction potential, Lee et al. [32] performed a comparative study of the ultracold collision dynamics of the He- H_2 system using the MR potential and a more recent ab initio potential developed by Boothroyd, Martin and Peterson (BMP) [33]. The BMP potential was considered to be an improvement, approaching chemical accuracy, over all conformations compared to the MR potential. However, significant differences were observed for vibrational relaxation of the $v = 1, j = 0$ state of the H_2 molecule in collisions with He computed using the two surfaces. The limiting value of the quenching rate coefficient on the BMP surface was found to be about three orders of magnitude larger than that of the MR surface. The difference was attributed to the more anisotropic nature of the BMP surface leading to larger values of the off-diagonal elements responsible for driving vibrational transitions. Indeed, it was found that the vibrational quenching of the $v = 1, j = 0$ level was dominated by the transition to the $v' = 0, j' = 8$ level which is driven by the high-order anisotropic terms of the interaction potential.

To explore the behavior of inelastic collisions involving polar molecules at ultracold temperatures, Balakrishnan, Forrey and Dalgarno [23] investigated vibrational and ro-

tational relaxation of CO in ^4He -CO collisions. The dynamics of the He-CO system was found to exhibit significantly different features at low temperatures compared to the He-H₂ system. Quantum scattering calculations of ^4He and ^3He collisions with the CO molecule revealed that the larger reduced mass and the deeper van der Waals interaction potential of the He-CO system give rise to a number of shape resonances in the energy dependence of vibrational relaxation cross sections [23, 24]. The effect of shape resonances on low temperature vibrational relaxation rate coefficients will be discussed in the next subsection. The computed values of vibrational relaxation rate coefficients for both ^3He and ^4He collisions with CO($v = 1$) have been found to be in good agreement with experimental data of Reid et al. [34] in the temperature range 35 – 100 K. Calculations of vibrational relaxation rate coefficients for the He-CO system in the temperature range 35 – 1500 K have also been reported by Krems [35]. He has shown that inclusion of the centrifugal distortion of the vibrational wavefunction enhances the relaxation process, and that the quenching rate coefficients are sensitive to high-order anisotropic terms in the angular expansion of the interaction potential [36].

Bodo, Gianturco and Dalgarno [37] have extended the work of Balakrishnan et al. [23] to study the vibrational relaxation of excited CO($v = 2, j = 0, 1$) molecules in collision with ^4He atoms at ultra-low energies. They found that vibrational quenching of CO($v = 2, j = 0, 1$) in collisions with ^4He is dominated by the $v = 2 \rightarrow v = 1$ transition. The cross sections for the $v = 2 \rightarrow v = 0$ transition were found to be about four orders of magnitude smaller than the single quantum transitions for both $j = 0$ and $j = 1$ initial rotational levels.

Ultracold vibrational relaxation of a number of other molecules in collisions with He atoms has been reported by a number of other investigators in recent years. Stoecklin, Voronin, and Rayez [38] reported the vibrational relaxation of F₂ in collisions with ^3He atoms. In this study, they constructed the PES of He-F₂ using *ab initio* points obtained by high-level molecular electronic-structure calculations, and reported the cross sections for elastic scattering and inelastic relaxation of F₂($v = 0, 1, j = 0$) for collision energies in the range 10^{-6} – 2000 cm⁻¹. A similar study has been reported by the same authors for the $^3\text{He} + \text{HF}(v = 0, 1, j = 0, 1)$ system [39]. The vibrational quenching cross sections were found to be very small compared to pure rotational quenching, in agreement with the results for the He-CO system. This is due to the weak dependence of the He-HF PES on the HF internuclear distance and the strong anisotropy of the interaction potential.

Bodo and Gianturco [40] presented a comparative study of vibrational relaxation of CO($v = 1, 2, j = 0$), HF($v = 1, 2, j = 0$) and LiH($v = 1, 2, j = 0$) in collisions with ^3He and ^4He atoms in the Wigner regime. The quenching rate coefficients were found to depend

strongly on the collision partner. They reported rate coefficients in the range 10^{-21} – 10^{-19} cm³ s⁻¹ for CO, 10^{-16} – 10^{-15} cm³ s⁻¹ for HF, and 10^{-14} – 10^{-11} cm³ s⁻¹ for LiH. The differences were attributed to the features of the intermolecular forces between the diatomic molecules and the He atoms. The interaction potential of the He-CO system is almost isotropic and is characterized by small vibrational couplings elements. The He-HF system is more anisotropic and the couplings between vibrational states are more significant. The interaction potential of the He-LiH system is very anisotropic and it exhibits strong vibrational couplings.

There is considerable ongoing experimental interest in cooling and trapping NH [41, 42] and OH [43, 44] molecules using the buffer gas cooling and Stark deceleration methods described in the chapters by Doyle and by Meijer. Krems et al. [45] and Cybulski et al. [46] reported cross sections and rate coefficients for elastic scattering and Zeeman relaxation in ^3He -NH collisions from ultralow energies to 10 cm⁻¹. The calculations were performed using the rigid rotor approximation and an accurate He-NH PES. It was demonstrated that the elastic scattering of NH molecules with He atoms in weak magnetic fields is at least five orders of magnitude faster than the Zeeman relaxation, which suggests that the NH molecule is a good candidate for buffer-gas cooling. In a related study González-Sánchez et al. [47] examined rotational relaxation and spin-flipping in collisions of OH with He atoms at ultralow energies. They found that the rotational relaxation processes dominate the elastic process as the collision energy is decreased to zero.

While theoretical prediction of rate coefficients for vibrational and rotational relaxation in a number of atom - diatom systems has been made, comparable experimental results are not available for majority of these systems. The first measurements of vibrational relaxation of molecules at temperatures below 1 K were reported by Weinstein et al. [48]. In their study, CaH molecules slowed down by elastic collisions with ^3He buffer gas atoms were trapped in an inhomogeneous magnetic field. An upper bound of the rate coefficients for spin-flipping transitions in CaH as well as vibrational relaxation of CaH molecules in the $v = 1$ vibrational level in collisions with ^3He atoms were estimated at a temperature of about 500 mK. Balakrishnan et al. [49] presented a theoretical analysis of the vibrational relaxation of CaH in collisions with ^3He atoms based on quantum close-coupling calculations and an *ab initio* PES for the He-CaH system developed by Groenenboom and Balakrishnan [50]. In a related study, Krems et al. [51] reported cross sections for spin-flipping transitions in CaH induced by collisions with ^3He and obtained results in close agreement with the experimentally derived values of Weinstein et al [48]. Krems et al. demonstrated that at low energies, spin-flipping transitions in the $N = 0$ rotational level of $^2\Sigma$

molecules induced by structureless atoms occur through coupling to the rotationally excited $N > 0$ levels and that the corresponding rate coefficients are determined by the spin-rotation interaction with the transiently rotationally excited molecule.

Table I provides a compilation of zero-temperature quenching rate coefficients for vibrational and rotational relaxation in a number of atom - diatom systems.

system	initial (v, j)	$k_{T=0}$ (cm^3s^{-1})	Ref.
H + H ₂	($v = 1, j = 0$)	1.0×10^{-17}	[28]
³ He + H ₂	($v = 1, j = 0$)	3×10^{-17}	[19]
	($v = 10, j = 0$)	3.6×10^{-14}	[19]
⁴ He + CO	($v = 1, j = 0$)	6.5×10^{-21}	[23]
	($v = 1, j = 1$)	9.0×10^{-19}	[23]
³ He + CO	($v = 1, j = 0$)	1.3×10^{-19}	[40]
	($v = 2, j = 0$)	2.1×10^{-19}	[40]
⁴ He + CO	($v = 1, j = 0$)	5.3×10^{-21}	[40]
	($v = 2, j = 0$)	1.3×10^{-20}	[40]
³ He + CaH	($v = 0, j = 1$)	3.5×10^{-12}	[49]
	($v = 1, j = 0$)	2.6×10^{-17}	[49]
³ He + HF	($v = 1, j = 0$)	3.1×10^{-16}	[40]
	($v = 2, j = 0$)	2.6×10^{-15}	[40]
⁴ He + HF	($v = 1, j = 0$)	8.1×10^{-16}	[40]
	($v = 2, j = 0$)	6.5×10^{-15}	[40]
³ He + LiH	($v = 1, j = 0$)	9.0×10^{-14}	[40]
	($v = 2, j = 0$)	3.6×10^{-12}	[40]
⁴ He + LiH	($v = 1, j = 0$)	3.8×10^{-13}	[40]
	($v = 2, j = 0$)	1.5×10^{-11}	[40]

TABLE I: Zero-temperature inelastic rate coefficients for different atom - molecule systems.

2. Shape resonances in molecular collisions

At energies above the onset of the s-wave regime, cross sections will be dominated by contributions from non-zero angular momentum partial waves. If the interaction potential includes an attractive part, the effective potentials for non-zero angular momentum partial waves may possess centrifugal barriers that introduce shape resonances in the collision energy dependence of the cross section. This is illustrated in Fig.4 for the vibrational relaxation of CO($v = 1, j = 0$) in collisions with ⁴He atoms.

The sharp features in the energy dependence of the cross section for energies between 0.1 and 10.0 cm^{-1} arises from shape resonances supported by the van der Waals interaction potential between He and the CO molecule. As shown in Fig.5, when integrated over the velocity distribution of the colliding species the shape resonances lead to significant enhancement of the vibrational

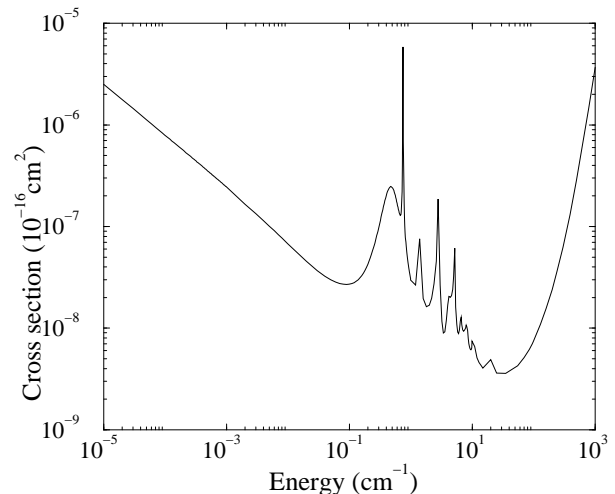


FIG. 4: Cross section for the quenching of the $v = 1, j = 0$ level of CO in collisions with ⁴He as a function of the incident kinetic energy. Reproduced with permission from Balakrishnan et al. [23].

relaxation rate coefficient for temperatures between 0.1 and 10.0 K. Similar results have been found for vibrational relaxation of CO [24], O₂[25], and CaH [49] in collisions with ³He atoms. The sharp features in the energy dependence of the vibrational relaxation cross sections for the Ar + D₂ system shown in Fig.2 also arises from shape resonances supported by the Ar–D₂ van der Waals potential. The effect is generally more pronounced for systems composed of heavier diatomic molecules and interaction potentials with deep van der Waals wells for which the density of states will be much higher leading to rich resonance structures in the cross sections.

3. Feshbach resonances in molecular collisions

Feshbach resonances occur in multichannel scattering in which an unbound (continuum) channel is coupled to a bound state of another channel. If the energy of the interacting system in the unbound channel lies close to that of the bound state and the coupling between the two channels is strong the cross section may change dramatically in the vicinity of the resonance. In the Feshbach resonance method for producing ultracold molecules, an external magnetic field is used to tune the energy of the bound pair to that of the separated atoms. In atom - diatom systems, the bound state may correspond to a quasibound state of the atom - diatom van der Waals complex. Channel potentials corresponding to different initial vibrational and rotational levels of the diatom may induce Feshbach resonances. For the He–CO system Feshbach resonances were found to occur near channel thresholds corresponding to the $j = 1$ rotational level

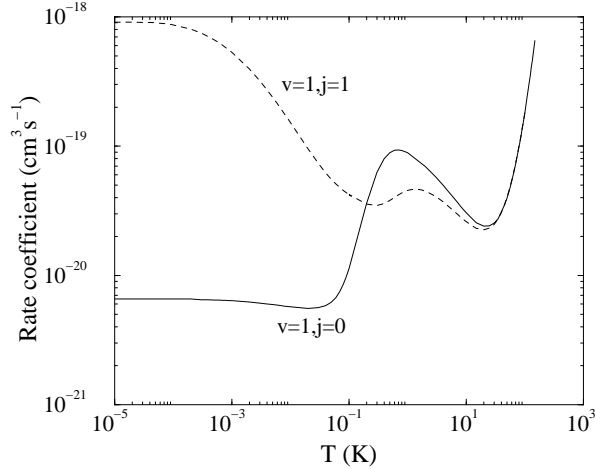


FIG. 5: Rate coefficients for the quenching of $\text{CO}(v=1, j=0, 1)$ by collisions with ^4He as functions of the temperature. Reproduced with permission from Balakrishnan et al. [23].

in the $v=0$ and $v=1$ vibrational levels. Fig. 6 shows the Feshbach resonance in the elastic scattering cross sections in the $v=1, j=0$ channel in the vicinity of the $v=1, j=1$ level. The presence of the Feshbach resonance close to the opening of the $j=1$ level has a dramatic effect on the vibrational quenching cross sections from the $v=1, j=1$ level of the CO molecule. Since the Feshbach resonance occurs so close to the threshold of the $v=1, j=1$ channel, its effect on scattering in the $v=1, j=1$ level is similar to that of the zero-energy resonance discussed previously for the $\text{Ar} + \text{D}_2$ system. This is illustrated in Fig. 5 (see also Table I) where we compare the rate coefficients for vibrational relaxation from the $v=1, j=0$ and $v=1, j=1$ levels of the CO molecule. The zero-temperature limiting value of the quenching rate coefficient of the $v=1, j=1$ level is about two orders of magnitude larger than for the $v=1, j=0$ level. Similar Feshbach resonances have also been shown to occur in the vibrational and rotational predissociation of $\text{He}-\text{H}_2$ van der Waals complexes [20]. Forrey et al. [20] has successfully used the effective range theory to predict the predissociation lifetimes of these resonances.

The Feshbach resonances can be used as a very sensitive probe for the interaction potential and also to selectively break or make bonds in chemical reactions. The coupling between the bound and unbound states can be modified by applying an external electric or magnetic field and this provides an important mechanism for creating or eliminating Feshbach resonances and thereby controlling the collisional outcome. Krems have shown that weakly bound van der Waals complexes can be dissociated by tuning a Feshbach resonance using an external magnetic field [52]. In this case the dissociation occurs through coupling between Zeeman levels of the bound

and unbound channels and the magnitude of the coupling is varied by changing the external magnetic field.

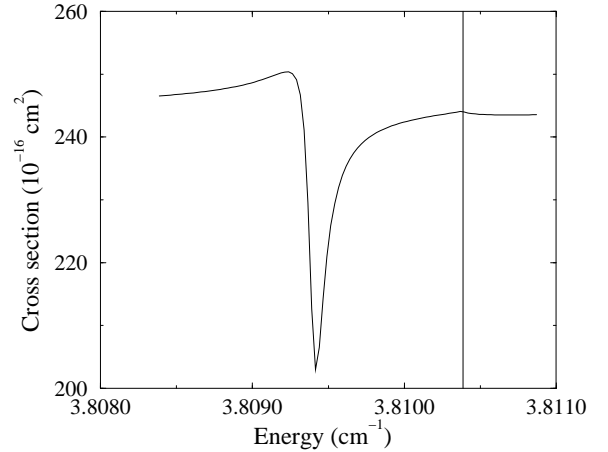


FIG. 6: Feshbach resonance in the elastic scattering cross section of $\text{CO}(v=1, j=0)$ by ^4He atoms. The resonance occurs just below the opening of the $v=1, j=1$ level shown by the vertical line. The energy is relative to the $v=1, j=0$ level of the CO molecule. Reproduced with permission from Balakrishnan et al. [23].

B. Quasi-resonant transitions

While the properties of cold and ultracold collisions are quite different from scattering at thermal energies and quantum effects dominate at low temperatures, a remarkable correlation between classical and quantum dynamics has been discovered in the relaxation of rotationally excited diatomic molecules. Experiments performed nearly two decades ago [53, 54] showed that collisions of rotationally excited diatomic molecules with atoms may result in very efficient internal energy transfer between specific rotational and vibrational degrees of freedom. The energy transfer becomes highly efficient when the collision time is longer than the rotational period of the molecule. This effect has since been termed “quasi-resonant rotation-vibration energy transfer”. The experimental results revealed that the quasi-resonant (QR) transitions satisfy the propensity rule $\Delta j = -4\Delta v$ or $\Delta j = -2\Delta v$ where $\Delta v = v_f - v_i$ and $\Delta j = j_f - j_i$ [53, 54]. This inelastic channel dominates over all other ro-vibrational transitions. The QR transfer is generally insensitive to details of the interaction potential. Rather, the QR process involves conservation of the action, $I = n_v v + n_j j$, where n_v and n_j are small integers. Forrey et al. [21] found that the QR transitions also occur in cold and ultracold collisions of rotationally excited diatomic molecules with atoms and that the process is largely insensitive to the details of the interaction potential even in the ultracold regime. The $\Delta j = -2\Delta v$ QR transition in $\text{He} + \text{H}_2$ collisions [55] is illustrated in Fig. 7

where the zero-temperature vibrational and rotational transition rate coefficients for different initial vibrational levels of the H_2 molecule are plotted as functions of the initial rotational level. For initial rotational levels greater than 12 the QR transition becomes the dominant energy transfer mechanism compared to pure rotational quenching. The gap at $j = 22$ occurs because the $\Delta j = -2\Delta v$ transition is energetically not accessible for this initial state at zero temperature. Forrey et al. [21] found that the QR process is even more dominant at low temperatures than at thermal energies. Remarkably, classical trajectory calculations [21] were successful in correctly predicting the correlation between Δj and Δv at ultracold temperatures even though the changes in v and j were fractional. Extensive studies of QR energy transfer in cold and ultracold temperatures have been reported by Forrey et al. [56–59]. Ruiz and Heller [60] have recently published a review paper providing a detailed analysis of QR phenomenon using semi-classical techniques. McCaffery and coworkers [61–63] have also reported a number of quasi-classical trajectory calculations of the QR process in thermal energy collisions and successfully interpreted a large body of experimental data based on the QR phenomenon and simple parametric models.

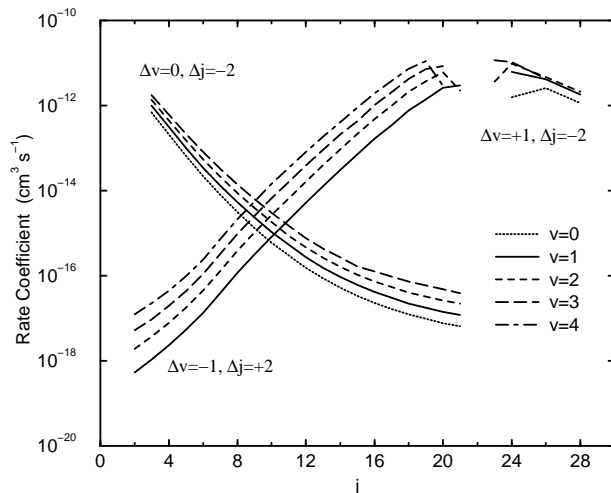


FIG. 7: Zero-temperature rate coefficients for $^4\text{He} + \text{H}_2(v, j)$ collisions as functions of the initial vibrational and rotational quantum numbers. Reproduced with permission from Forrey et al. [55].

C. Atom - molecular ion collisions

Dynamics of ionic systems are different from collisions of neutral species. The short-range part of the interaction potential for ionic systems is usually more anisotropic and the long-range part has an attractive component

which is determined by the polarizability of the atom and it vanishes as $1/R^4$ where R is the atom - molecule center-of-mass distance [64]. Due to the strong polarizability term, the interaction potential for ionic systems extends to longer range compared to neutral atom - molecule systems. Therefore, it is important to understand the effect of both the short and long range part of the interaction potential on the scattering dynamics. For this purpose, several studies have focused on ultracold collisions between molecular ions and neutral atoms as well as neutral molecules and atomic ions.

Bodo et al. [64] investigated rotational quenching in $\text{Ne}_2^+ + \text{Ne}$ and $\text{He}_2^+ + \text{He}$ collisions at ultra-low energies. They found that the Wigner regime begins at a collision energy of 10^{-4} cm^{-1} for the He system and 10^{-6} cm^{-1} for the Ne system. In general, the s-wave Wigner regime was found to occur at lower energies for ionic systems compared to neutral species. For example, in $\text{He} + \text{H}_2$ [19] and $\text{He} + \text{O}_2$ [25] collisions the Wigner regime begins at collision energies of about 10^{-2} cm^{-1} . The differences are attributed to the long range of the ion - neutral interaction potential which enhances contributions from higher partial waves. The differences between the He and Ne systems can be attributed to the mass difference and to the strength of the long range interaction potentials. For the heavier Ne system the long range part is more attractive, which increases the contribution of higher-order partial waves at ultra-low energies. The magnitude of the zero-energy rate coefficients for rotational quenching in these molecular ions is on the order of $10^{-9} \text{ cm}^3 \text{ s}^{-1}$, which is considerably larger than for collisions involving neutral species.

Stoecklin et al. [65] have performed a comparative study of collisions of $\text{N}_2^+(v = 1, j = 0)$ molecular ions with neutral ^3He or ^4He atoms, and the scattering of neutral $\text{N}_2(v = 1, j = 0)$ molecules in collisions with ^3He or ^4He atoms. The vibrational quenching cross sections for these systems are presented in Fig. 8. While the behavior of the quenching cross sections of neutral N_2 molecules with ^3He and ^4He atoms was found to be similar, they observed a striking difference between the quenching cross sections of N_2^+ in collisions with ^3He and ^4He atoms. In particular, the resonance positions in the quenching cross sections were significantly shifted and the number of resonances was different. The $\text{N}_2^+ + ^3\text{He}$ system has a shape resonance at a collision energy of 10^{-2} cm^{-1} which is absent for the $\text{N}_2^+ + ^4\text{He}$ system. Furthermore, the zero-energy quenching rate coefficient is an order of magnitude larger for collisions of $\text{N}_2^+(v = 1, j = 0)$ with ^3He than with ^4He , whereas it is comparable for collisions of $\text{N}_2(v = 1, j = 0)$ with both ^3He and ^4He . The differences may be due to a virtual state in the $\text{N}_2^+(v = 1, j = 0) + ^3\text{He}$ collision system. More recently, Guillon et al. [66] studied the effect of spin-rotation interaction on vibrational and rotational quenching for the $\text{He}-\text{N}_2^+$ system. They found that the vibrational quenching is not modified by

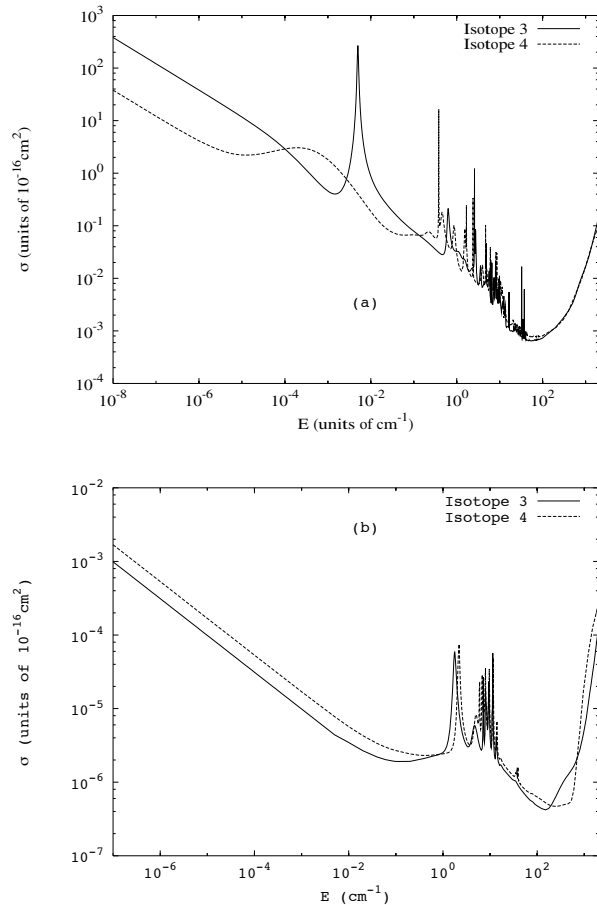


FIG. 8: Vibrational quenching cross sections for $\text{N}_2^+(v=1, j=0) + {}^3\text{He}$ and $\text{N}_2^+(v=1, j=0) + {}^4\text{He}$ (upper panel) and $\text{N}_2(v=1, j=0) + {}^3\text{He}$ and $\text{N}_2(v=1, j=0) + {}^4\text{He}$ (lower panel) systems. Reproduced with permission from Stoecklin et al. [65].

the spin-rotation coupling, while rotational transitions are sensitive to the fine-structure interactions.

Table II provides a compilation of zero-temperature quenching rate coefficients for vibrational and rotational relaxation in several ion atom - molecule systems.

III. CHEMICAL REACTIONS AT ULTRACOLD TEMPERATURES

The last three decades have seen impressive progress in the experimental and theoretical descriptions of chemical reactions between atoms and small molecular systems. While fully state-resolved experiments have been performed for a large number of collision systems, accurate quantum dynamics calculations have been restricted to systems involving light atoms such as $\text{H} + \text{H}_2$, $\text{F} + \text{H}_2$, $\text{Cl} + \text{H}_2$, $\text{C} + \text{H}_2$, $\text{N} + \text{H}_2$, $\text{O} + \text{H}_2$ and some of their

system	initial (v, j)	$k_{T=0}$ (cm^3s^{-1})	Ref.
$\text{Ne}_2^+ + \text{Ne}$	$(v=0, j=2)$	3.3×10^{-10}	[64]
	$(v=0, j=4)$	7.3×10^{-10}	[64]
	$(v=0, j=6)$	7.0×10^{-10}	[64]
$\text{He}_2^+ + \text{He}$	$(v=0, j=2)$	6.7×10^{-10}	[64]
	$(v=0, j=4)$	8.4×10^{-10}	[64]
	$(v=0, j=6)$	1.2×10^{-9}	[64]
$\text{N}_2^+ + {}^3\text{He}$	$(v=1, j=0)$	4×10^{-14}	[65]
$\text{N}_2^+ + {}^4\text{He}$	$(v=1, j=0)$	3×10^{-15}	[65]

TABLE II: Zero-temperature inelastic rate coefficients for different ion atom - molecule systems.

isotopic analogues [67, 68]. Most experimental studies of small molecular systems focussed on reactions at thermal or elevated collision energies though some recent measurements have been extended to temperatures as low as 10 K for some astrophysically relevant systems [69]. Due to the possibility of achieving coherent chemistry there has been substantial interest in understanding the behavior of chemical reactions at cold and ultracold temperatures. At these temperatures perturbations introduced by external electric and magnetic fields are significant compared to the collision energies involved and external fields can be employed to control and manipulate the reaction outcome. Over the last seven years a number of studies of ultracold atom - diatom chemical reactions have been reported both for reactions with and without an energy barrier. Chemical reactions at low temperatures often behave quite differently from reactions at elevated temperatures. In particular, the weak van der Waals interaction potential which does not play any significant role at high temperatures may have a dramatic effect on the outcome of reactions at low temperatures.

A. Tunneling dominated reactions

In the course of the last 10 – 15 years there has been much interest in understanding the role of resonances in chemical reactions that involve an energy barrier for which the reactivity is primarily driven by tunneling at low temperatures. Recent studies on $\text{F} + \text{H}_2/\text{HD}/\text{D}_2$ [11, 70–80], $\text{Cl} + \text{HD}$ [81, 82], $\text{H} + \text{HCl}/\text{DCI}$ [83], $\text{Li} + \text{HF} / \text{LiF} + \text{H}$ [84, 85], $\text{O} + \text{H}_2$ [86, 87], and $\text{F} + \text{HCl}/\text{DCI}$ [88] reactions have demonstrated that decay of quasibound states of the van der Waals interaction potential in the entrance and exit channels may give rise to narrow Feshbach resonances in the cross sections.

The reactions of F with H_2 and HD have been the subject of numerous quantum scattering calculations over the last two decades. The two reactions have emerged as benchmark systems for experimental and theoretical studies of resonances in chemical reactions. A de-

tailed analysis of the low energy resonance features in the $F + H_2$ reaction was presented by Castillo et al. in 1996 [70]. They demonstrated that several resonances that appear in the energy dependence of the cumulative reaction probability for the $F + H_2$ reaction arise due to the van der Waals interaction potential in the product $HF + H$ channel. In particular, the origin of the resonances has been attributed to the van der Waals potential associated with the $HF(v' = 3, j' = 0 - 3)$ channels. A large number of experimental and theoretical papers has appeared which examined various aspects of these resonance features [11, 70–72, 75–80]. Among these studies, the work of Takayanagi and Kurosaki [71] deserves special attention. They showed that for $F + H_2$, $F + HD$ and $F + D_2$ reactions reactive scattering resonances occur due to the decay of quasibound states of the van der Waals potential in the entrance channel of the reaction. These Feshbach resonances are associated with the decay of quasibound states of adiabatic potentials corresponding to $F \cdots H_2(v = 0, j = 0, 1)$, $F \cdots HD(v = 0, j = 0 - 2)$, and $F \cdots D_2(v = 0, j = 0 - 2)$ complexes, obtained by diagonalizing the $J = 0$ Hamiltonian in a basis set of the asymptotic ro-vibrational states of the reactant molecules.

1. Reactions at zero temperature

Balakrishnan and Dalgarno [11] showed that quasibound states of the $F + H_2$ van der Waals complex have a dramatic effect on the reactivity in the Wigner threshold regime. They found that the $F + H_2(v = 0, j = 0)$ reaction has a rate coefficient of $1.25 \times 10^{-12} \text{ cm}^3 \text{ s}^{-1}$ in the zero-temperature limit. Their calculation was based on the widely used PES of Stark and Werner [89] for the $F + H_2$ system. The relatively large value of the zero-temperature rate coefficient is due to the presence of a small narrow energy barrier for the reaction so that tunneling of the H atom is efficient. The vibrational level resolved cross sections for the $F + H_2(v = 0, j = 0)$ reaction are shown in Fig. 9 for the total angular momentum quantum number $J = 0$. The $v' = 2$ level is the dominant channel at low energies in agreement with the behavior at higher energies.

Subsequent calculations showed that at low energies the $F + HD$ reaction is dominated by the formation of the HF product with an HF/DF branching ratio of about 5.5 [74]. The formation of the DF product is suppressed because tunneling of the heavier D atom is less efficient. In earlier quantum calculations, Baer and coworkers [90, 91] reported HF/DF branching ratios ranging from 1.5 at 450 K to 6.0 at 100 K. Their low temperature value is in close agreement with the zero-temperature limit obtained by Balakrishnan and Dalgarno [74]. Fig. 10 compares the $J = 0$ cross sections for the $F + H_2(v = 0, j = 0)$ and $F + HD(v = 0, j = 0)$ reactions over a kinetic energy range of 10^{-7} to 1.0 eV.

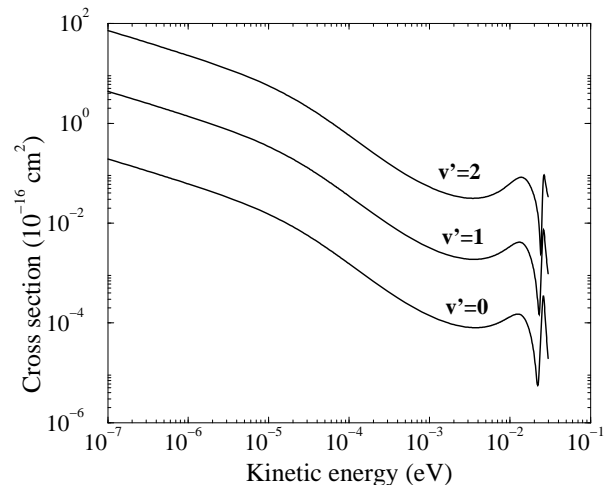


FIG. 9: $J = 0$ cross sections for $F + H_2(v = 0, j = 0) \rightarrow HF(v') + H$ reaction for $v' = 0 - 2$ as functions of the incident kinetic energy. Reproduced with permission from Balakrishnan and Dalgarno [11].

In the Wigner threshold regime, the reactivity of the $F + H_2$ system is an order of magnitude greater than that of the $F + HD$ reaction. A rigorous analysis of the scattering resonances in the $F + HD$ reaction was recently presented by De Fazio et al. [80], who provided a detailed characterization of the resonances supported by the entrance and exit channels of the van der Waals potential and discussed the effect of higher total angular momenta on the position and lifetime of the resonances. Stereodynamical aspects of the $F + H_2$ collision and the effect of polarization of the H_2 molecule on the outcome of the reaction at low energies were recently explored by Aldegunde et al. [77]. They argued that a reactant polarization scheme can be exploited to control state-to-state dynamics of the reaction.

To explore the role of tunneling in chemical reactions at cold and ultracold temperatures Bodo, Gianturco, and Dalgarno [73] investigated the dynamics of the $F + D_2$ system at low and ultra-low energies. They found that compared to the $F + H_2$ reaction, the reactivity of $F + D_2$ is significantly suppressed in the Wigner regime with an HF/DF ratio of about 100. This is illustrated in Fig. 11 where the $J = 0$ cumulative reaction probability and cross sections for the $F + H_2$ and $F + D_2$ reactions are plotted as functions of the incident kinetic energy from the Wigner limit to 0.01 eV.

The dramatic suppression of the $F + D_2$ reaction in the Wigner regime cannot be explained based on tunneling alone. A closer examination of the reaction probabilities for the $F + H_2$ and $F + D_2$ reaction revealed that an unusual enhancement of the reactivity occurs for the $F + H_2$ reaction at about 3×10^{-5} eV [75] (see the upper panel

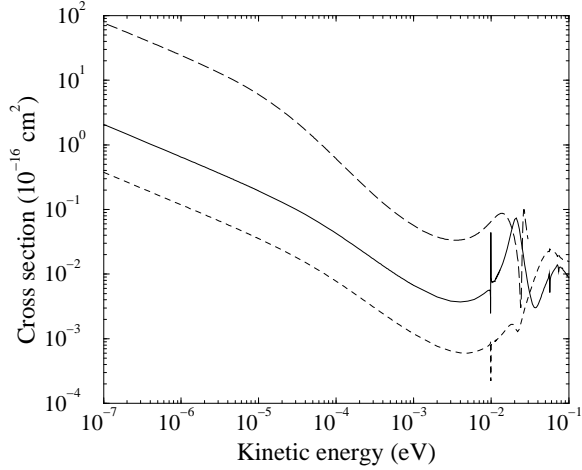


FIG. 10: Comparison of $J = 0$ cross sections for $\text{F} + \text{HD}(v = 0, j = 0) \rightarrow \text{HF} + \text{D}$ (solid curve), $\text{F} + \text{HD}(v = 0, j = 0) \rightarrow \text{DF} + \text{H}$ (short-dashed curve) and $\text{F} + \text{H}_2(v = 0, j = 0) \rightarrow \text{HF} + \text{H}$ (long-dashed curve) reactions as functions of the incident kinetic energy. Reproduced with permission from Balakrishnan and Dalgarno [74].

of Fig. 11). This feature was attributed to the presence of a virtual state. The enhancement of the limiting value of the rate coefficient for the $\text{F} + \text{H}_2$ reaction was also ascribed to the virtual state. Evidence for the virtual state is the presence of a Ramsauer–Townsend minimum in the elastic cross section at an energy of about 3×10^{-5} eV and a negative value of the real part of the scattering length for the $\text{F} + \text{H}_2$ reaction [75].

To explore how isotope substitution modifies reactivity at low temperatures Bodo et al. [75] artificially varied the mass of the hydrogen atoms in the calculation for the $\text{F} + \text{H}_2$ reaction from 0.5 to 1.5 amu. As illustrated in Fig. 12, for an H atom mass of 1.12 amu the virtual state induces a zero energy resonance at which the real part of the scattering length diverged to infinity. For the same value of the H atom mass, the zero-temperature rate coefficient of the reaction attains a value of $1.0 \times 10^{-9} \text{ cm}^3 \text{ s}^{-1}$ which is about three orders of magnitude larger than that of the $\text{F} + \text{H}_2$ reaction in the Wigner limit. The variation of the scattering length of the $\text{F} + \text{H}_2$ system as a function of the mass of the pseudo-hydrogen atom is similar to the variation of scattering length as a function of the magnetic field in the vicinity of a Feshbach resonance.

Another example of a tunneling dominated reaction is the $\text{Li} + \text{HF} \rightarrow \text{LiF} + \text{H}$ reaction. At cold and ultracold temperatures the reaction occurs by tunneling of the relatively heavy fluorine atom. The $\text{LiH} + \text{F}$ channel is energetically not accessible at low energies and tunneling of the H atom is not involved in this reaction at low temperatures. Due to strong electric dipole forces ex-

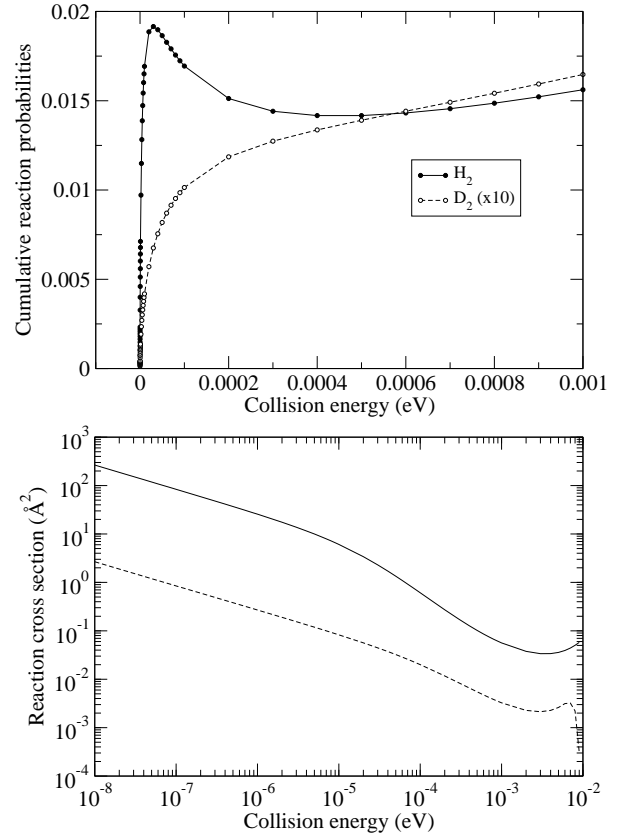


FIG. 11: Comparison of the $J = 0$ cumulative reaction probabilities (upper panel) and cross sections (lower sub-panel) of $\text{F} + \text{H}_2$ and $\text{F} + \text{D}_2$ reactions as functions of the incident kinetic energy. Reproduced with permission from Bodo et al. [75].

erted by the HF molecule, the van der Waals interaction potential of the LiHF system is deeper compared to the $\text{F} + \text{H}_2$ system. The $\text{Li} \cdots \text{HF}$ van der Waals potential well is about 0.24 eV (1936.0 cm^{-1}) and the $\text{H} \cdots \text{LiF}$ potential well is about 0.07 eV (565.0 cm^{-1}). Quantum scattering calculations for $\text{Li} + \text{HF}$ and $\text{LiF} + \text{H}$ reactions by Weck and Balakrishnan [84, 85] with the PES of Aguado et al. [92] have shown that for incident energies below 10^{-3} eV the reaction cross section exhibits a large number of resonances. The energy dependence of the $J = 0$ cross section for $\text{Li} + \text{HF}(v = 0, j = 0)$ collisions is shown in Fig. 13. Detailed bound state calculations of the LiHF van der Waals complexes revealed that for the $\text{Li} + \text{HF}(v = 0, j = 0)$ reaction the resonances correspond to the decay of $\text{Li} \cdots \text{HF}(v = 0, j = 1 - 4)$ van der Waals complexes. Calculations with vibrationally excited HF molecules showed that the reaction becomes about 600 times more efficient in the Wigner regime when HF is excited to the $v = 1$ vibrational level. As seen in Fig. 13, a unique feature of the $\text{Li} + \text{HF}(v = 0, j = 0)$ reaction is the presence of a strong peak at 5.0×10^{-4} eV at which the reaction cross section is about six orders of magnitude larger than the background cross section. The

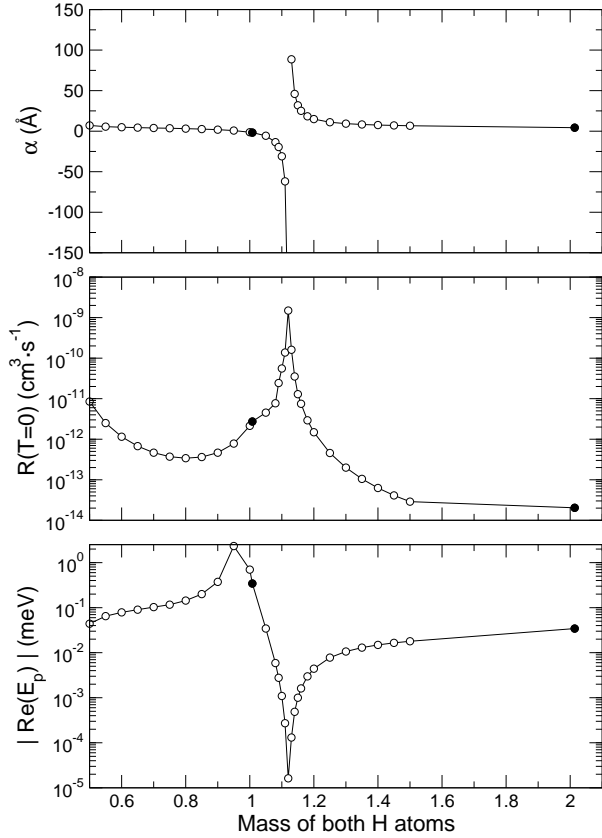


FIG. 12: Real part of the scattering length (upper panel), zero-temperature limiting values of the rate coefficient (middle panel), and positions of quasibound states (lower panel) of the $\text{F} \cdots \text{H}_2$ complex as functions of the mass of a pseudo hydrogen atom. Reproduced with permission from Bodo et al. [75].

results for both $\text{Li} + \text{HF}$ [84] and $\text{LiF} + \text{H}$ [85] reactions with thermal and non-thermal vibrational excitation suggest that heavy-atom tunneling may play an important role in chemical reactions at cold and ultracold temperatures. An experimental study [12] of an organic ring expansion reaction at 8 K has shown that the reaction occurs almost exclusively by carbon tunneling. The tunneling contribution was found to be orders of magnitude greater than over the barrier contribution. In a recent work, Tscherbil and Krems [93] have explored the $\text{Li} + \text{HF}$ and $\text{LiF} + \text{H}$ reactions in the presence of an external electric field. They have shown that, for temperatures below 1 K, the reaction probability can be significantly influenced by electric fields.

2. Feshbach resonances in reactive scattering

Van der Waals complexes formed during collisions can either undergo vibrational predissociation or vibrational prereaction leading to sharp features in the energy dependence of the cross sections. The term “prereaction”

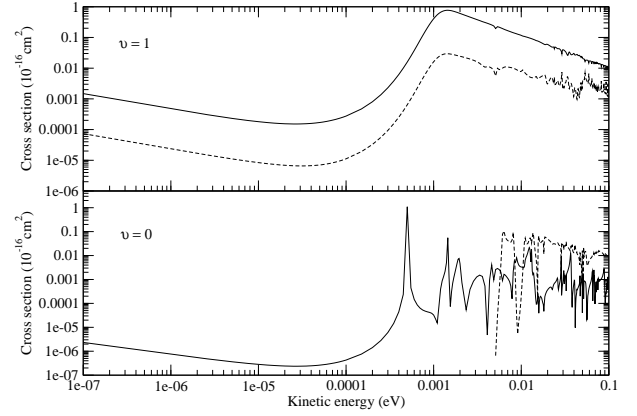


FIG. 13: Cross sections for LiF formation (solid curve) and non-reactive scattering (dashed curve) in $\text{Li} + \text{HF}(v, j = 0)$ collisions as functions of the incident kinetic energy: results for $v = 0$ (lower panel); results for $v = 1$ (upper panel). Reproduced with permission from Weck and Balakrishnan [84].

refers to the process in which a rotationally or vibrationally excited van der Waals complex decays through chemical reaction rather than by rotational or vibrational predissociation. For reactions with energy barriers the chemical reaction pathway may involve tunneling. The reactions of Cl with H_2 and HD are dominated by tunneling at low temperatures [81–83]. Compared to the $\text{F} + \text{H}_2$ and $\text{F} + \text{HD}$ reactions, the energy barrier for the $\text{Cl} + \text{H}_2$ reaction is much larger and the reactivity at low energies is significantly suppressed. Nearly a decade ago, Skouteris et al. [81] showed that the van der Waals interaction potential between Cl and HD determines the reaction outcome, despite the fact that the depth of the van der Waals interaction potential for the $\text{Cl} \cdots \text{HD}$ system is less than one-tenth of the height of the reaction barrier. Quantum scattering calculations of the $\text{Cl} + \text{HD}$ reaction on PESs without the van der Waals interaction potential predict nearly equal probabilities for HCl and DCl products [81]. However, if the potential surface includes the van der Waals interaction a strong preference for the DCl product occurs at thermal energies, in agreement with experimental results. The effect of these weakly bound states on the reactivity at cold and ultracold temperatures has recently been explored by Balakrishnan [82].

The cross sections for HCl and DCl formation and non-reactive rovibrational transitions in $\text{Cl} + \text{HD}(v = 1, j = 0)$ collisions for total angular momentum quantum number $J = 0$ are shown in Fig. 14 as functions of the total energy [82]. The sharp features in the cross sections correspond to Feshbach resonances arising from the decay of quasibound van der Waals complexes formed in the entrance channel of the reaction. The quasibound states can be identified by examining bound states of adiabatic potentials correlating with the $v = 1, j = 0$ and $v = 1, j = 1$ levels of the HD molecule. They are

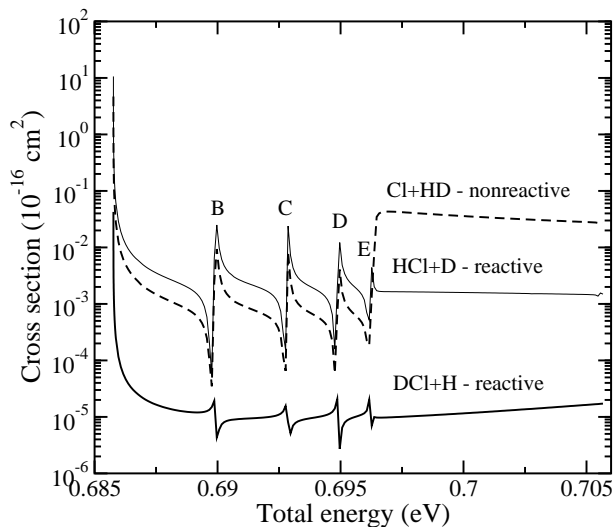


FIG. 14: Reactive and non-reactive scattering cross sections for $\text{Cl} + \text{HD}(v=1, j=0)$ reaction as functions of the incident kinetic energy. Reproduced with permission from Balakrishnan [82].

displayed in Fig. 15 as functions of the atom - molecule separation. The adiabatic potential curves are computed by diagonalizing the diabatic potential energy matrix obtained in a basis set of rovibrational levels of the HD molecule at each value of the atom - molecule separation. The Feshbach resonances labeled B, C, D, and E in Fig. 14 result from the decay of the corresponding quasibound states shown in Fig. 15.

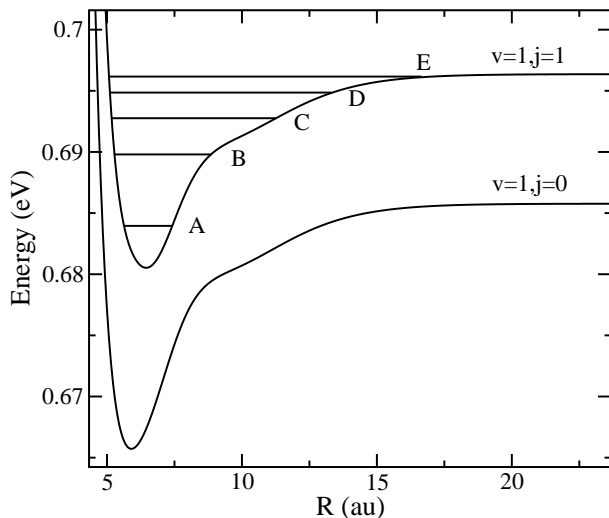


FIG. 15: Adiabatic potential energy curves of the $\text{Cl} + \text{HD}$ system correlating with the $\text{HD}(v=1, j=0)$ and $\text{HD}(v=1, j=1)$ levels as functions of the atom - molecule separation. Quasibound levels responsible for the resonances in Fig. 14 are labeled by B, C, D, and E. Reproduced with permission from Balakrishnan [82].

The cross sections in Fig. 14 do not show a peak corresponding to the metastable state A. This is because the state A is too deeply bound and it is not accessible through scattering in the $v=1, j=0$ channel. Fig. 14 also shows that the quasibound states preferentially undergo prereaction than predissociation. This is due to the enhanced coupling of the resonance states with the reactive channels compared to those with the non-reactive channels. The wavefunctions of quasibound states B and E are shown in Fig. 16 as functions of the atom - molecule separation. Although the wavefunction of the weakly bound state E extends far beyond the transition state region of the reaction, it preferentially undergoes prereaction compared to predissociation. Thus, regions of the interaction potential far away from the transition state region may have a significant effect on reactivity especially when part of the wavefunction in that region is sampled by a resonance state which is coupled to the reactive channel. Fig. 14 also demonstrates that since the reaction is dominated by tunneling at low temperatures the formation of the $\text{DCl} + \text{H}$ product which involves the tunneling of the D atom is severely suppressed in the threshold regime. This is more clearly illustrated in Fig. 4 of Ref. [82] where the reaction cross section is plotted as a function of the incident kinetic energy.

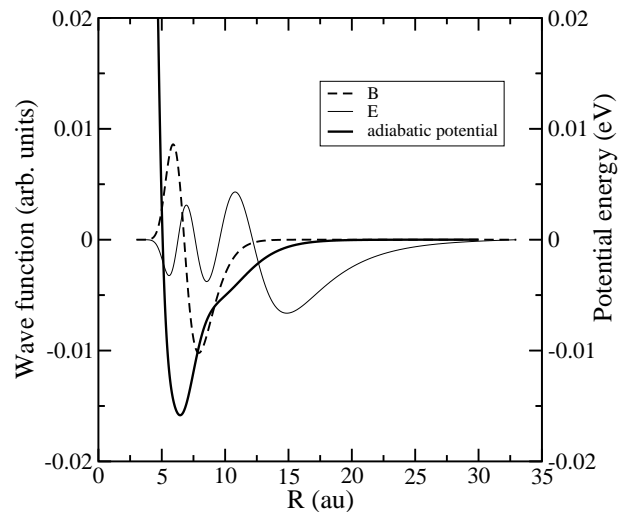


FIG. 16: Adiabatic potential and the wavefunctions of the quasibound levels B and E shown in Fig. 15 as functions of the atom - molecule separation. Amplitudes of the wavefunctions have been reduced by a factor of 10 for the convenience of plotting. Reproduced with permission from Balakrishnan [82].

Table III provides a compilation of zero-temperature quenching rate coefficients for a number of atom - diatom chemical reactions which are dominated by tunneling at low energies.

system	initial (v, j)	$k_{T=0}$ (cm^3s^{-1})	Ref.
F + H ₂	$(v = 0, j = 0)$	1.3×10^{-12} (H + HF)	[11]
F + HD	$(v = 0, j = 0)$	2.8×10^{-14} (D + HF)	[74]
	$(v = 0, j = 0)$	0.5×10^{-14} (H + DF)	[74]
F + D ₂	$(v = 0, j = 0)$	2.1×10^{-14} (D + DF)	[37]
F + HCl	$(v = 0, j = 0)$	1.2×10^{-17} (Cl + HF)	[88]
F + HCl	$(v = 1, j = 0)$	4.0×10^{-15} (Cl + HF)	[88]
		5.3×10^{-15} (F + HCl)	[88]
F + HCl	$(v = 2, j = 0)$	5.2×10^{-13} (Cl + HF)	[88]
		3.3×10^{-13} (F + HCl)	[88]
F + DCl	$(v = 1, j = 0)$	4.4×10^{-21} (Cl + DF)	[88]
H + HCl	$(v = 0, j = 0)$	2.4×10^{-19} (Cl + H ₂)	[83]
	$(v = 1, j = 0)$	7.2×10^{-14} (Cl + H ₂)	[83]
	$(v = 2, j = 0)$	1.9×10^{-11} (Cl + H ₂)	[83]
H + DCl	$(v = 1, j = 0)$	7.8×10^{-15} (Cl + HD)	[83]
	$(v = 2, j = 0)$	1.7×10^{-12} (Cl + HD)	[83]
Cl + HD	$(v = 1, j = 0)$	1.7×10^{-13} (D + HCl)	[82]
		7.1×10^{-16} (H + DCl)	[82]
		7.8×10^{-14} (Cl + HD)	[82]
Li + HF	$(v = 0, j = 0)$	4.5×10^{-20} (H + LiF)	[84]
	$(v = 1, j = 0)$	2.8×10^{-17} (H + LiF)	[84]
H + LiF	$(v = 1, j = 0)$	3.8×10^{-15} (Li + HF)	[85]
		1.6×10^{-14} (H + LiF)	[85]
	$(v = 2, j = 0)$	1.7×10^{-14} (Li + HF)	[85]
		2.7×10^{-13} (H + LiF)	[85]

TABLE III: Zero-temperature quenching rate coefficients for tunneling dominated reactions. The final arrangement has also been specified.

B. Barrierless reactions

1. Collision systems of three alkali metal atoms

As discussed by Hutson and Soldán in two recent reviews [6, 14], progress on the production of ultracold molecules and the creation of molecular Bose–Einstein condensates of alkali-metal systems have motivated theoretical studies on ultracold atom - dimer alkali-metal collisions. Here, we give an overview of recent calculations for spin-polarized triatomic alkali-metal systems, Li + Li₂ [94–97], Na + Na₂ [98, 99] and K + K₂ [100]. These results have all been obtained using the reactive scattering code written by Launay and Le Dourneuf [101], based on a time-independent quantum formalism. Refs. [94, 95, 97, 100] describe the details of the PESs and dynamics calculations. The quantum dynamics studies of Refs. [98, 99] have been performed using the Na₃ PES reported by Higgins et al. [102], while the results of Ref. [96] have been obtained using the Li₃ PES calculated by Colavecchia et al. [103]. Another PES for Li₃ has been constructed by Brue et al. [104].

Quantum scattering calculations show that ultracold

reactions of alkali metal atoms with alkali metal dimers are much more efficient than tunneling driven processes. This can be explained based on the following considerations. First, the indistinguishability of the atoms may play a role. For a homonuclear triatomic system, the three possible arrangement channels are the same. Also the presence of identical two-body potentials in all three arrangement channels may enhance the depth of the three-body interaction potential. Consider the two-body term (additive term) of a homonuclear triatomic system at equilateral geometries. Since the distances between the three identical atoms are the same, the same diatomic potential term is added three times to yield the two-body terms of the triatomic system. If the diatomic potential is deep or repulsive, the two-body term will be three times deeper or repulsive at equilateral geometries. In contrast, for triatomic systems with distinguishable atoms, the diatomic pairs are not the same. For example, for the Li + HF system, the three diatomic fragments are distinctly different. They have completely different electronic structures and properties such as minima, equilibrium distances, turning points, and the nature and range of the interaction. Thus, at an equilateral configuration for which the three diatomic distances are the same but the diatomic potential energies are different (one may be attractive while the other two may be repulsive), the overall two-body term can be weaker than the individual two-body interaction potential. This could lead to a triatomic interaction region that is less strong than that of a homonuclear triatomic system.

Second, the topology of the PES plays a significant role. For all alkali-metal trimer systems, the minimum energy configurations arise at equilateral and collinear geometries as shown by Soldán et al. [105]. Furthermore, the surface is barrierless so that all atom - dimer alkali-metal collisional approaches are energetically possible. In contrast, most of the non-alkali systems discussed above are characterized by a collinear (or bend) atom - diatom approach, and dominated by a repulsive barrier in the triatomic transition-state region. The particular topology of the PES arises from the three-body interaction potential. Also, the couplings between different electronic surfaces of the triatomic system give rise to conical intersections, which create a repulsive barrier in the transition-state region. If the energy barrier is high and its width large, tunneling will be very inefficient leading to very small values for the reaction rate coefficients in the Wigner regime. Although reactivity can be enhanced when resonances are present, the background scattering in reactive cross sections is generally quite small. In contrast, for almost all alkali-metal trimer systems, the conical intersections arise at small interatomic distances where the PES is sufficiently repulsive that it plays no significant role at ultra-low energy and the reactivity is not influenced by such repulsive barriers.

Third, the density of states of the system plays an important role. If the density of states is small as for light systems, the typical energy spacing is rather large.

For heavy systems such as alkali-metal systems, the density of states is very large and the narrow energy spacing can lead to very strong couplings, especially in the vicinity of avoided crossings. The strong couplings will lead to efficient energy transfer between different quantum states. This may also explain the relatively weak dependence of the vibrational quenching rate coefficients on the initial vibrational state of the molecule in atom - dimer alkali-metal collisions.

Fig. 17 provides a comparison between elastic and quenching rate coefficients for $^{39}\text{K} + ^{39}\text{K}_2(v = 1, j = 0)$ [100] collisions at energies ranging from 10^{-9} K to 10^{-2} K. The results include contributions from the total angular momentum quantum numbers $J = 0 - 5$. For low vibrational states of the K_2 dimer, quenching processes are more efficient than elastic scattering at ultracold energies. For example, at a temperature of 10^{-9} K, the quenching rate coefficient is about $10^{-10} \text{ cm}^3 \text{ s}^{-1}$ compared to $10^{-13} \text{ cm}^3 \text{ s}^{-1}$ for elastic scattering. The quenching processes lead to collisional relaxation of the molecules to lower ro-vibrational states resulting in trap loss.

Similar results have been obtained for $\text{Na} + \text{Na}_2$ [98, 99] and $\text{Li} + \text{Li}_2$ [94, 96, 97] collisions. The zero-energy quenching rate coefficients for these systems are found to be on the order of $10^{-11} - 10^{-10} \text{ cm}^3 \text{ s}^{-1}$. The quenching processes are more efficient than the elastic collisions at ultracold temperatures. Thus, quenching of vibrationally excited alkali-metal dimers in collisions with alkali-metal atoms occurs with significant rates at ultracold temperatures. The typical magnitude of these rate coefficients from the scattering calculations is in reasonable agreement with experimental results. In a recent experiment, Staunum et al. [106] reported a value of $9.8 \times 10^{-11} \text{ cm}^3 \text{ s}^{-1}$ for the relaxation of low-lying vibrational levels of Cs_2 in collisions with Cs atoms at a temperature of 60×10^{-6} K. In a separate experiment, Zahzam et al. [107] determined a quenching rate coefficient of $2.6 \times 10^{-11} \text{ cm}^3 \text{ s}^{-1}$ for the same system at a temperature of 40×10^{-6} K. Wynar et al. [108] estimated inelastic rate coefficients of $8 \times 10^{-11} \text{ cm}^3 \text{ s}^{-1}$ for $\text{Rb} + \text{Rb}_2$ collisions. Mukaiyama et al. [109] reported an inelastic rate coefficient of $5.5 \times 10^{-11} \text{ cm}^3 \text{ s}^{-1}$ for collisions of Na atoms with Na_2 molecules created by the Feshbach resonance method while Syassen et al. [110] obtained a value of $2 \times 10^{-10} \text{ cm}^3 \text{ s}^{-1}$ for collisions of Rb atoms with Rb_2 molecules.

At large atom - diatom separations, R , the interaction potential can be approximated by an effective potential, composed of a repulsive centrifugal term and the long range interaction potential. For alkali-metal trimer systems, the atom - diatom long range potential is a van der Waals interaction potential and behaves as $-C_6/R^6$. The classical capture model (also known as the Langevin model) has been shown to work quite well for these systems [100] at certain energy regimes. The Langevin

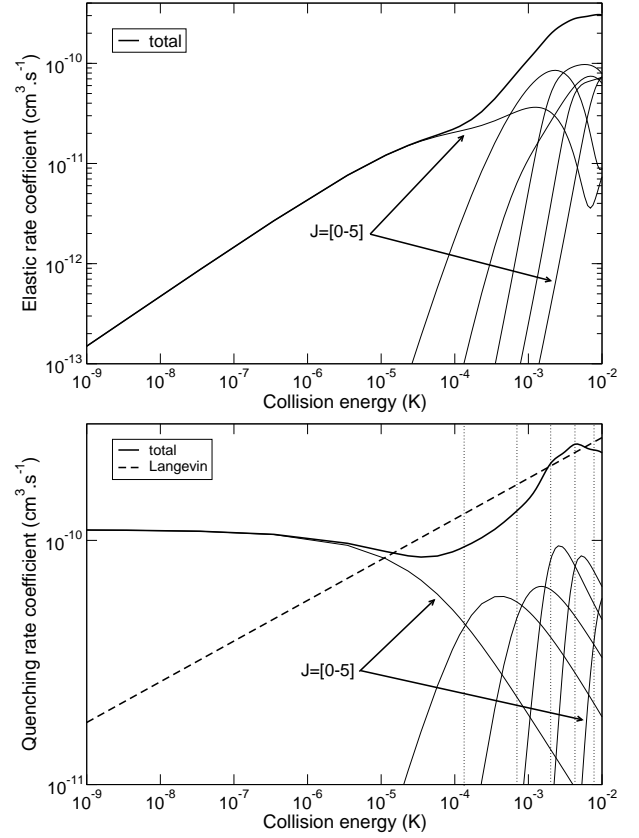


FIG. 17: Elastic (upper panel) and quenching (lower panel) rate coefficients versus the collision energy for $^{39}\text{K} + ^{39}\text{K}_2(v = 1, j = 0)$ scattering. The rate coefficient from a capture model is also shown for the quenching processes. Adapted with permission from Quémener et al. [100].

model is based on the assumption that if the total energy of the system can overcome the effective barrier, then the elastic probability is zero and the quenching probability is one. Otherwise, the elastic probability is one and the quenching probability is zero. Classically, the barrier prevents the atom and the molecule from accessing the region of strong coupling with the other channels.

Results obtained using the Langevin model for the $\text{K} + \text{K}_2$ system are shown in Fig. 17 along with the quantum results. As Fig. 17 illustrates, three different regions can be distinguished for the $\text{K} + \text{K}_2$ system. The first region, for collision energies below 10^{-6} K, corresponds to the Wigner regime where the threshold laws apply. In this regime, the quenching rate coefficient tends to a constant while the elastic component approaches zero as the square root of the collision energy. A quantum description is required and classical models cannot describe the dynamics in this regime. The second region, above a collision energy of 10^{-3} K, corresponds to the Langevin regime. Here, the difference between the full quantum calculation and the classical model is within 10 %. Similar results have been found for $^7\text{Li} + ^7\text{Li}_2(v = 1, 2, j = 0)$ and $^6\text{Li} + ^6\text{Li}_2(v = 1, 2, j = 1)$ collisions by Cvitaš et

al. [94], who showed that in the Langevin regime the rate coefficients become independent of the vibrational level of the molecule. The third region is intermediate between the Wigner and Langevin regimes, which typically corresponds to a quantum calculation with two or three partial waves. As shown in the lower panel of Fig. 17 the height of each J -resolved effective barrier depicted by vertical lines for $J = 1 - 5$ corresponds approximately to the maximum of each J -resolved quenching rate coefficient. This indicates that the quenching process becomes significant when the barrier height is energetically overcome. Whenever the elastic and quenching rate coefficients have comparable values, the Langevin regime is reached, as shown in Fig. 17. Since the quenching probability is almost equal to one and the elastic probability is almost equal to zero, elastic and quenching transition matrix elements are both equal to one and the cross sections and rate coefficients for the two processes become similar.

The above analysis shows that at energies above the onset of the Wigner regime the Langevin model can correctly describe the dynamics for barrierless atom - dimer alkali-metal collisions because of the strong inelastic couplings. However, the classical model is not suitable for tunneling dominated reactions. Accurate quantum dynamics calculations are computationally demanding for heavier systems such as Cs + Cs₂, Rb + Rb₂, Rb + RbCs or Cs + RbCs and the classical model may be used to qualitatively describe the dynamics of these systems at energies above the s-wave regime. The temperature dependence of the rate coefficients predicted by the Langevin model is given by the simple formula in atomic units:

$$k_{\text{Lang}}(T) = \pi \left(\frac{8k_B T}{\pi \mu} \right)^{1/2} \left(\frac{2C_6}{k_B T} \right)^{1/3} \Gamma(2/3)$$

where μ is the reduced mass of the atom - diatom collisional system and C_6 the dominant atom - diatom long range coefficient. In Fig. 18 we show the rate coefficients predicted by the Langevin model as functions of the temperature for different atom - diatom and diatom - diatom collisions involving Rb or Cs atoms. For Rb-RbCs, Cs-RbCs, and RbCs-RbCs collisions we used the corresponding C_6 coefficients calculated by Hudson et al. [111]. In the absence of similar data for Cs + Cs₂ and Rb + Rb₂ collisions, we approximated the atom - dimer C_6 coefficient by multiplying the corresponding atom - atom value by a factor of two. For Cs + Cs₂ collisions we used the C_6 coefficient for Cs-Cs interaction calculated by Amiot et al. [112] and for Rb + Rb₂ collisions we adopted the C_6 coefficient for Rb-Rb interaction reported by Derevianko et al. [113]. As shown in Fig. 18 the Langevin model predicts rate coefficients within an order of magnitude of the experimental values for the different systems. The predicted results for the Cs + Cs₂, Rb + RbCs, and Cs + RbCs collisions agree with the corresponding experimental data of Refs. [106, 107, 111] within the reported error bars. For Rb + Rb₂ collisions the Langevin model

predicts results in very close agreement with the experimental result of Wynar et al. [108]. Thus, the Langevin model appears to be valid for describing collisional properties of these systems at μK temperatures. The model also confirms that cold and ultracold collisions of alkali metal atoms and dimers are essentially characterized by the leading term in the long-range part of the interaction potential.

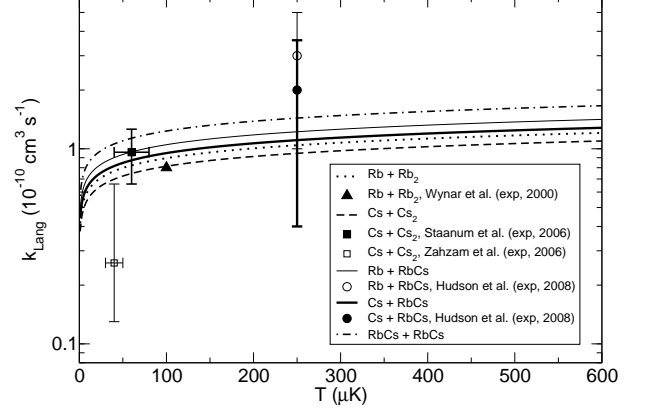


FIG. 18: Rate coefficients as functions of the temperature predicted by the Langevin model compared with experimental data for different collisional processes involving Rb or Cs atoms. The curves correspond to the Langevin results and the symbols denote the experimental results.

2. Role of PES in determining ultracold reactions

Potential energy surfaces are the key ingredients that enter in quantum dynamics calculations. While the two-body terms are generally well known and accurate, the three-body terms are more difficult to compute with high precision since they are non-additive and involve correlations between the three atoms. As a consequence, quantum dynamics calculations may suffer from the quality and degree of accuracy of the three-body terms. The sensitivity of the ultracold collision cross sections to the details of the PES has been investigated for atom - dimer alkali-metal systems by Quémener et al. [99] for Na + Na₂($v = 1 - 3, j = 0$) and by Cvitaš et al. [97] for Li + Li₂($v = 0 - 3, j = 0$). In these studies, a linear scaling factor λ has been included to tune the three-body interaction term in the PES and cross sections were calculated as a function of λ . Other studies have compared the dynamics with and without the three-body terms for Na + Na₂($v = 1, j = 0$) [98] and for Li + Li₂($v = 0 - 10, j = 0$) [96] collisions.

The dependence of the total quenching cross sections on the three body term for Na + Na₂($v = 1 - 3, j = 0$) scattering [99] at a collision energy of 10^{-9} K is shown in Fig. 19. The contribution of each final vibrational level is also plotted. For the $v = 1$ vibrational level, the cross sections are very sensitive to the details of the three-body

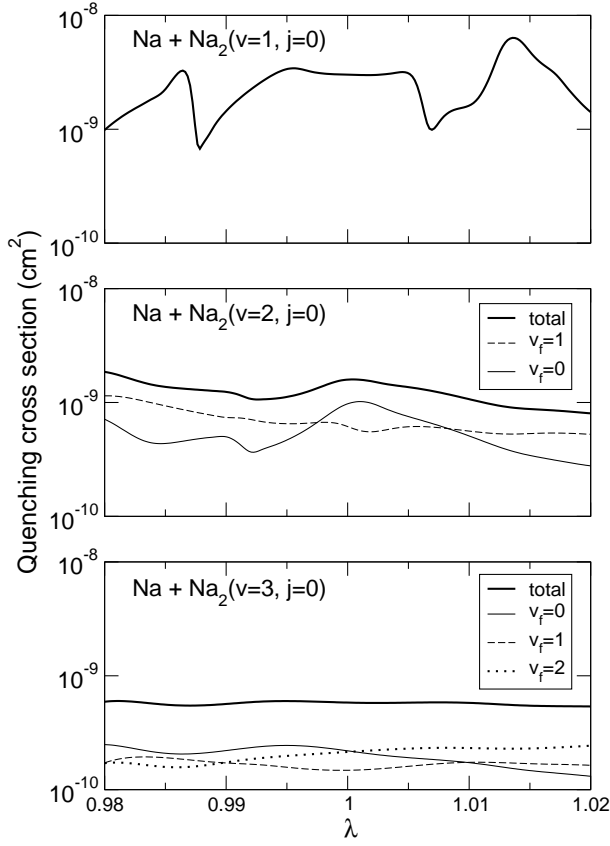


FIG. 19: Dependence of the quenching cross sections on the three-body term at a collision energy of 10^{-9} K for $\text{Na} + \text{Na}_2(v = 1 - 3, j = 0)$. Reproduced with permission from Quémener et al. [99].

potential. A change of 1 % in λ leads to a significant change of 75 % in the cross sections. At the minimum of the Na_3 potential, a change of 1 % corresponds approximately to 10 K. At present, ab initio calculations of PESs cannot be done with such accuracy. Thus it appears that it is difficult to get an accuracy better than two orders of magnitude in the cross sections for $\text{Na} + \text{Na}_2(v = 1, j = 0)$ collisions. However, for $v = 2$ and 3, the total cross sections show a weaker dependence on the three-body term. The state-resolved cross sections do not show strong dependence on the three-body term, compared to collisions of molecules in $v = 1$.

Fig. 20 shows the dependence of the state-to-state cross sections on the three body term for the reaction $\text{Na} + \text{Na}_2(v = 3, j = 0) \rightarrow \text{Na} + \text{Na}_2(v_f = 2, 1, 0, j_f)$ at a collision energy of 10^{-9} K. The oscillations in the cross sections, when λ is modified, are due to Feshbach resonances which arise when a triatomic quasibound state (or a virtual state) crosses the energy threshold as the strength of the interaction potential is decreased (increased). When such a Feshbach resonance occurs, Cvitaš et al. [97] have argued, strong resonant peaks appear in the cross sections if inelastic couplings are weak. In contrast, weak oscillations of one order of magnitude at best appear

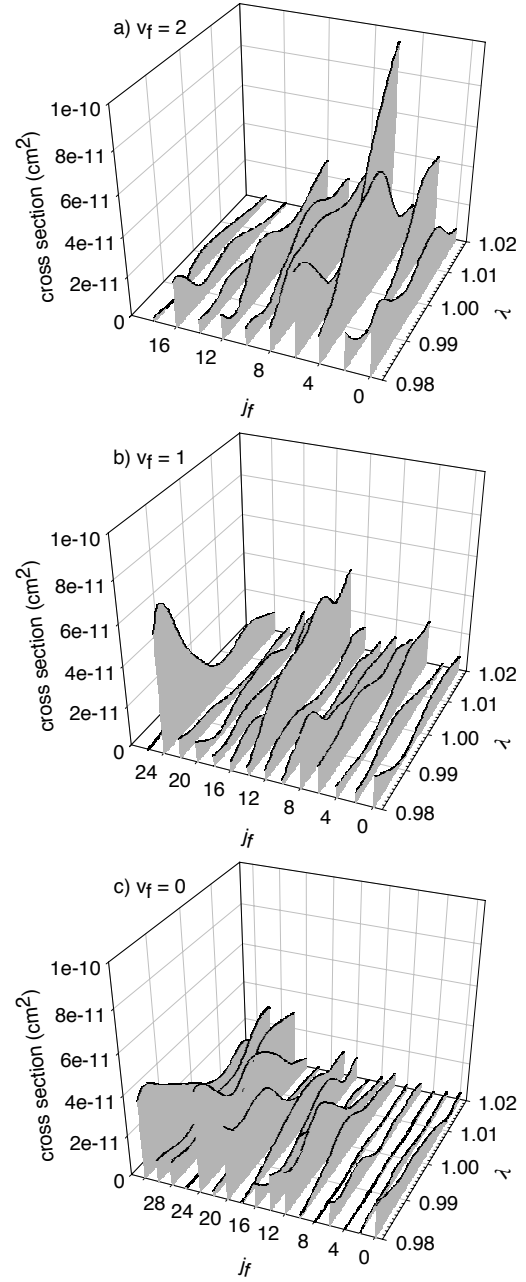


FIG. 20: Variation of state-to-state cross sections at a collision energy of 10^{-9} K for $\text{Na} + \text{Na}_2(v = 3, j = 0) \rightarrow \text{Na} + \text{Na}_2(v_f = 2, 1, 0, j_f)$ as a function of the parameter λ . See text for details. Reproduced with permission from Quémener et al. [99].

when inelastic couplings are strong, as in alkali-metal trimer systems. A generalization of this effect has been discussed by Hutson [114]. Larger modifications of the three-body term affect the cross sections significantly. This can also be seen in Fig. 21 for $\text{Li} + \text{Li}_2$ collisions [96] in which the three-body term is excluded from the dynamics calculation. The state-to-state cross sections exhibit a stronger dependence on the three body term.

3. Relaxation of vibrationally excited alkali metal dimers

Ultracold diatomic molecules produced in photoassociation or Feshbach resonance methods are usually created in excited vibrational states. Theoretical studies involving highly vibrationally excited molecules are challenging due to the large number of energetically open reaction channels present in the quantum calculation. This puts severe restriction on the calculations for vibrationally excited molecules at low temperatures. Ultracold quantum dynamics calculations for collisions of highly vibrationally excited molecules have been reported in 2007 by Quémener et al. [96] for the $\text{Li} + \text{Li}_2$ system. A three-atom problem is generally described by two different kinds of asymptotic channels. The first kind are the single-continuum states (SCSs). They correspond to configurations where the triatomic system dissociates asymptotically into an atom and a diatomic molecule. The second kind are the double-continuum states (DCSs). They correspond to configurations where the triatomic system dissociates asymptotically into three separated atoms. Since highly vibrationally excited molecular states lie close to and below the triatomic dissociation limit, they are also coupled with the DCSs which lie above the dissociation limit. As a consequence, DCSs have to be included in quantum simulations of atom - diatom systems involving highly vibrationally excited diatomic molecules [96]. This dramatically increases the size and complexity of the quantum dynamics problem.

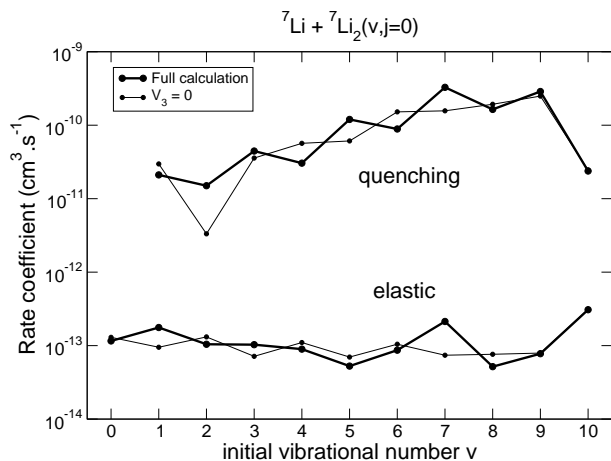


FIG. 21: Dependence of the elastic and quenching rate coefficients on the vibrational excitation of the molecule for ${}^7\text{Li} + {}^7\text{Li}_2(v = 0 - 10, j = 0)$ scattering at a collision energy of 10^{-9} K. The bold line corresponds to the full calculation and the thin line corresponds to the calculation without the three-body term of the PES. Adapted with permission from Quémener et al. [96].

Figure 21 shows the dependence of the rate coefficients for ${}^7\text{Li} + {}^7\text{Li}_2(v = 0 - 10, j = 0)$ collisions on

the vibrational quantum number at a collision energy of 10^{-9} K [96]. Quenching processes are more efficient than the elastic scattering for both high and low vibrational levels. Similar results have been found for ${}^6\text{Li} + {}^6\text{Li}_2(v = 0 - 9, j = 1)$ [96] system composed of fermionic atoms. Quenching rate coefficients show a slight decrease when the molecule is in its highest vibrational state. This is because the overlap of the wavefunctions of highly excited diatomic molecules with low-lying vibrational levels is very small leading to small values for the interaction potential coupling matrix elements between the initial and final states [115]. These results do not directly apply to ultracold molecules composed of fermionic atoms created near a Feshbach resonance. In these experiments, the quenching processes are suppressed because the atom - atom scattering length is tuned to large and positive values leading to efficient Pauli blocking mechanism, as explained by Petrov et al. [116]. In the theoretical study of $\text{Li} + \text{Li}_2$ collisions, the atom - atom scattering length is small and negative and no suppression of the quenching processes is found for the molecule in the last vibrational state. Thus, the sign and magnitude of the Li-Li scattering length play a crucial role in the mechanism that suppresses quenching collisions.

The quenching rates displayed in Fig. 21 show an irregular dependence on the vibrational state of the molecule. This has already been seen for $\text{H} + \text{H}_2$ collisions [28, 117]. In contrast, experimental measurements of quenching rate coefficients for $\text{Cs} + \text{Cs}_2$ collisions [106, 107] do not show any dependence on the vibrational state of the molecule. The differences between these systems can be explained based on the following considerations.

First, the theoretical study applies to spin-polarized atom - dimer alkali-metal systems whereas it is not the case for the experiment. A full theoretical treatment should involve the electronic and nuclear spins of the alkali metal atoms as well as couplings between electronic surfaces of different spins. This is beyond the scope of quantum dynamics calculations at present and will involve significant new code development and massive computational efforts.

Second, the dynamics of the two systems are different. The lithium system is lighter and has a more attractive three-body term than the cesium system [105]. The triatomic adiabatic potential energy curves are well separated for a light system such as Li_3 and very dense for a heavy system such as Cs_3 . The density of states strongly influences the nature of vibrational relaxation. The effect of the density of states has been illustrated in calculations for the $\text{Li} + \text{Li}_2$ system which exclude the three-body term. Removing the three-body term makes the energy levels more sparse. This results in a more regular and monotonic dependence of the rate coefficients on the vibrational levels $v = 3 - 9$ as illustrated in Figure 21. This conclusion is in agreement with a previous work of Bodo et al. [117] for the $\text{H} + \text{H}_2$ system. When they

increased the density of states of the triatomic system, they found no significant dependence on the vibrational states of the molecule. However, for $v = 10$, they obtained the same results with and without the three-body term. The three-body term thus appears to be less significant for collisions of molecules in high vibrational levels. Since the three-body term vanishes at large separations it is only important in the short-range interaction region while high vibrational states involve spatially extended molecules and sample the long range part of the interaction potential. Therefore, three-body terms, which are the most difficult interaction energy terms to compute numerically for triatomic systems, may be neglected to a first approximation in dynamics of highly vibrationally excited molecules.

In the experiments, rate coefficients have been measured for temperatures of 40×10^{-6} K [107] and 60×10^{-6} K [106] for Cs + Cs₂ while the theoretical rate coefficients for Li + Li₂ were reported for a temperature of 10^{-9} K which corresponds to the Wigner threshold regime. Thus, it is likely that the experimental measurements did not probe the limiting values of the rate coefficients in the Wigner regime.

4. Reactions of heteronuclear and isotopically substituted alkali-metal dimer systems

Reactive collisions involving heteronuclear molecules are currently of great interest. A major goal of recent experiments has been to produce heteronuclear alkali-metal dimers in their electronic ground state. Examples include RbCs [111, 118, 119], NaCs [120, 121], KRb [122, 123], LiCs [124], and mixed isotopes ⁶Li⁷Li [125]. Quantum dynamics calculations for heteronuclear systems are more difficult. They are more interesting from a chemistry perspective because the reactive channels in collisions of heteronuclear molecules can be distinguished from inelastic channels.

Cvitaš et al. [95, 97] have explored the quantum dynamics of ⁷Li + ⁶Li⁷Li($v = 0, j = 0$), ⁷Li + ⁶Li₂($v = 0, j = 1$), ⁶Li + ⁷Li₂($v = 0, j = 0$), and ⁶Li + ⁶Li⁷Li($v = 0, j = 0$) collisions. The $J = 0$ cross sections for elastic scattering and chemical reactions in collisions of ⁷Li with ⁶Li⁷Li($v = 0, j = 0$) are presented in the upper panel in Fig. 22 for a wide range of collision energies. The cross sections are believed to be converged for energies up to 10^{-4} K. The reactive process which leads to ⁶Li + ⁷Li₂($v = 0, j = 0$) dominates over the elastic scattering at ultralow energies. However, the reactive process is less efficient than the vibrational relaxation process in homonuclear alkali systems discussed above. For instance, at a collision energy of 10^{-9} K, the ratio of the cross sections for reactive and elastic collisions is about two orders of magnitude for the heteronuclear system presented in Fig. 22 whereas it is about three orders of magnitude for homonuclear systems. Cvitaš et al. at-

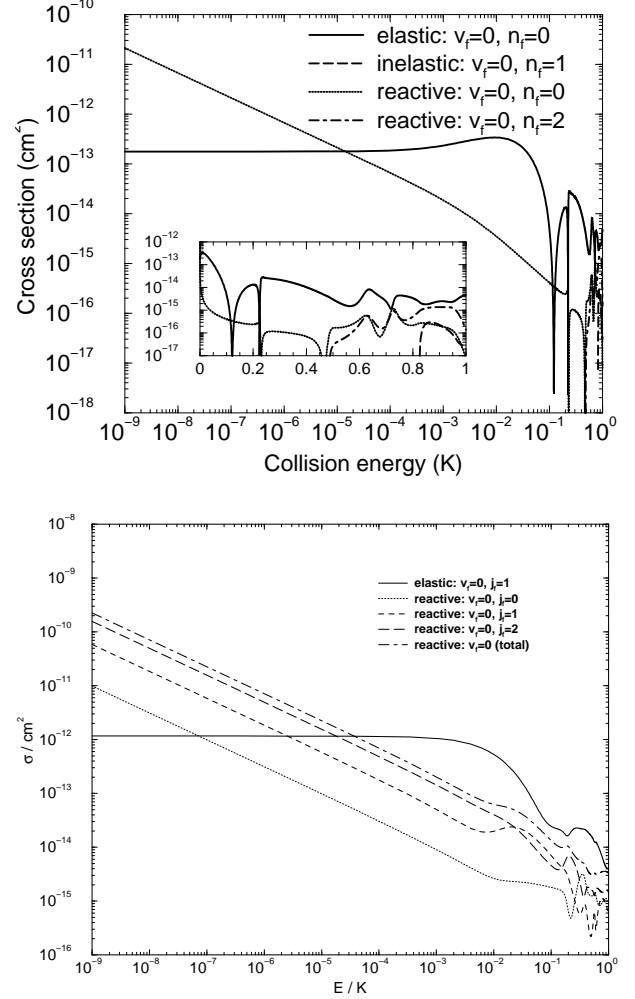


FIG. 22: Elastic and reactive s-wave cross sections for ⁷Li + ⁶Li⁷Li($v = 0, j = 0$) (upper panel) and ⁷Li + ⁶Li₂($v = 0, j = 1$) (lower panel). Reproduced with permission from Cvitaš et al. [95].

tributed the smaller ratio to the presence of only one open channel in the heteronuclear reaction.

The $J = 1$ elastic and reactive cross sections for ⁷Li + ⁶Li₂($v = 0, j = 1$) collisions are presented in the lower panel of Fig. 22. The reactive process leading to the formation of ⁶Li⁷Li molecules is slightly more efficient than elastic scattering in the Wigner regime. The other possible collision processes are ⁶Li + ⁶Li⁷Li($v = 0, j = 0$) and ⁶Li + ⁷Li₂($v = 0, j = 0$). However, only elastic scattering occurs in these systems at ultralow collisions energies.

These results provide important implications for the experiments on the production of ⁶Li⁷Li in an ultracold mixture of ⁶Li and ⁷Li atoms. Cvitaš et al. proposed to remove quickly the ⁷Li atomic gas after the formation of the ⁶Li⁷Li molecules in their ground state to prevent

the destructive reactive processes. But keeping the ${}^6\text{Li}$ atomic gas is recommended for sympathetic cooling of the ${}^6\text{Li}{}^7\text{Li}$ molecules since only elastic collisions are possible. Removing the ${}^6\text{Li}$ atoms will leave the fermionic heteronuclear ${}^6\text{Li}{}^7\text{Li}$ molecules in the trap. In the absence of ${}^6\text{Li}$ atoms, evaporative cooling by collisions between fermionic ${}^6\text{Li}{}^7\text{Li}$ molecules will not be effective since s-wave collisions of identical fermionic dimers will be suppressed due to the Pauli exclusion principle.

Table IV provides a compilation of zero-temperature quenching rate coefficients for different alkali-metal trimer systems.

IV. INELASTIC MOLECULE - MOLECULE COLLISIONS

Many of the studies of cold and ultracold molecules have focused on reactive and non-reactive scattering in atom - molecule collisions. At high densities of trapped molecules, molecule - molecule collisions need to be considered. The presence of rotational and vibrational degrees of freedom in both collision partners make molecule - molecule systems especially interesting. However, quantum dynamics calculations of molecule - molecule collisions are significantly more challenging. Most dynamical calculations of molecule - molecule scattering have relied on the rigid rotor approximation and some recent studies have adopted the coupled-states approximation. Calculations performed at high collision energies have employed more approximate methods based on semi-classical techniques. Here, we present a brief account of recent dynamical calculations for the $\text{H}_2 + \text{H}_2$ system and discuss some ongoing work on full-dimensional quantum calculations of ro-vibrational transitions in $\text{H}_2\text{--H}_2$ collisions. A brief discussion of hyperfine transitions in molecule - molecule systems is also provided for the illustrative examples of the $\text{O}_2 + \text{O}_2$ and $\text{OH} + \text{OH} / \text{OD} + \text{OD}$ systems.

A. Molecules in the ground vibrational state

The $\text{H}_2 + \text{H}_2$ system is the simplest neutral tetra-atomic system and it serves as a prototype for describing collisions between diatomic molecules. Though there have been a number of experimental and theoretical studies over the past several years on the $\text{H}_2 + \text{H}_2$ system (see Ref. [126] and references therein), only a few studies have explored the collision dynamics in the cold and ultracold regime.

Forrey [127] presented a study of rotational transitions in $\text{H}_2(v = 0, j = 2) + \text{H}_2(v' = 0, j' = 2)$ collisions at cold and ultracold collision energies using a rigid rotor model. He calculated the real and imagi-

system	initial (v, j)	$k_{T=0}$ (cm^3s^{-1})	Ref.
${}^{39}\text{K} + {}^{39}\text{K}_2$	$(v = 1, j = 0)$	1.1×10^{-10}	[100]
${}^{40}\text{K} + {}^{40}\text{K}_2$	$(v = 1, j = 1)$	8.0×10^{-11}	[100]
${}^{41}\text{K} + {}^{41}\text{K}_2$	$(v = 1, j = 0)$	9.8×10^{-11}	[100]
${}^7\text{Li} + {}^7\text{Li}_2$	$(v = 1, j = 0)$	2.1×10^{-11}	[96]
	$(v = 2, j = 0)$	1.5×10^{-11}	[96]
	$(v = 3, j = 0)$	4.4×10^{-11}	[96]
	$(v = 4, j = 0)$	3.0×10^{-11}	[96]
	$(v = 5, j = 0)$	1.2×10^{-10}	[96]
	$(v = 6, j = 0)$	8.9×10^{-11}	[96]
	$(v = 7, j = 0)$	3.3×10^{-10}	[96]
	$(v = 8, j = 0)$	1.6×10^{-10}	[96]
	$(v = 9, j = 0)$	2.9×10^{-10}	[96]
	$(v = 10, j = 0)$	2.4×10^{-11}	[96]
${}^6\text{Li} + {}^6\text{Li}_2$	$(v = 1, j = 1)$	3.3×10^{-11}	[96]
	$(v = 2, j = 1)$	2.0×10^{-11}	[96]
	$(v = 3, j = 1)$	5.1×10^{-11}	[96]
${}^7\text{Li} + {}^7\text{Li}_2$	$(v = 1, j = 0)$	5.6×10^{-10}	[94]
	$(v = 2, j = 0)$	9×10^{-11}	[94]
${}^6\text{Li} + {}^6\text{Li}_2$	$(v = 1, j = 1)$	2.8×10^{-10}	[94]
	$(v = 2, j = 1)$	4×10^{-10}	[94]
${}^{23}\text{Na} + {}^{23}\text{Na}_2$	$(v = 1, j = 0)$	2.9×10^{-10}	[99]
	$(v = 2, j = 0)$	1.1×10^{-10}	[99]
	$(v = 3, j = 0)$	6.1×10^{-11}	[99]
${}^7\text{Li} + {}^6\text{Li}{}^7\text{Li}$	$(v = 0, j = 0)$	4.1×10^{-12}	[97]
	$(v = 1, j = 0)$	2.1×10^{-10}	[97]
	$(v = 2, j = 0)$	4.4×10^{-10}	[97]
	$(v = 3, j = 0)$	4.0×10^{-10}	[97]
${}^7\text{Li} + {}^6\text{Li}_2$	$(v = 0, j = 1)$	4.4×10^{-11}	[97]
	$(v = 1, j = 1)$	5.2×10^{-10}	[97]
	$(v = 2, j = 1)$	2.6×10^{-10}	[97]
	$(v = 3, j = 1)$	3.0×10^{-10}	[97]
${}^6\text{Li} + {}^6\text{Li}{}^7\text{Li}$	$(v = 1, j = 0)$	2.6×10^{-10}	[97]
	$(v = 2, j = 0)$	3.5×10^{-10}	[97]
	$(v = 3, j = 0)$	4.4×10^{-10}	[97]
${}^6\text{Li} + {}^7\text{Li}_2$	$(v = 1, j = 0)$	2.8×10^{-10}	[97]
	$(v = 2, j = 0)$	5.3×10^{-10}	[97]
	$(v = 3, j = 0)$	4.6×10^{-10}	[97]

TABLE IV: Zero-temperature quenching rate coefficients for different atom - dimer alkali metal systems.

nary components of the complex scattering length for $\text{H}_2(v = 0, j = 2, 4, 6, 8) + \text{H}_2(v' = 0, j' = j)$ collisions and showed that the imaginary parts decrease with increasing j, j' . The imaginary parts of the scattering lengths are found to be small compared to the real parts, leading to small inelastic cross sections. Maté et al. [128] reported an experimental study of the rate coefficient for the $\text{H}_2(v = 0, j = 0) + \text{H}_2(v' = 0, j' = 0) \rightarrow \text{H}_2(v_f = 0, j_f = 0) + \text{H}_2(v'_f = 0, j'_f = 2)$ transition at temperatures between 2 K and 110 K. They found

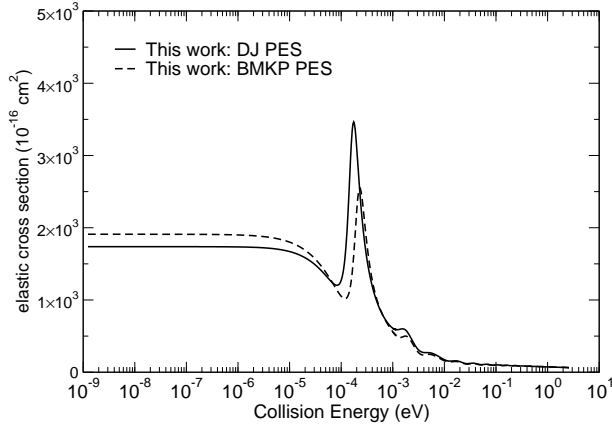


FIG. 23: Elastic cross section of $\text{H}_2(v=0, j=0) + \text{H}_2(v'=0, j'=0)$ as a function of the collision energy. Reproduced with permission from Lee et al. [126].

good agreement between the experimental results and quantum dynamics calculations based on the rigid rotor model using a PES reported by Diep and Johnson (DJ) [129]. Montero et al. [130] have investigated cold inelastic collisions of $n\text{-H}_2$ molecules in the ground vibrational state, using a 3:1 gas mixture of ortho and para hydrogen. They obtained good agreement between the experimental data and the theoretical calculations based on the DJ PES.

Using a quantum formalism based on the rigid rotor model, Lee et al. [126] have recently presented a comparative analysis of cross sections for rotationally-inelastic collisions between H_2 molecules at low and ultra-low energies. The elastic cross sections for $\text{H}_2(v=0, j=0) + \text{H}_2(v'=0, j'=0)$ collisions obtained in this study are presented in Fig. 23 for two different PESs. The limiting value of the elastic scattering cross section in the ultra-low energy regime is $1.91 \times 10^{-13} \text{ cm}^2$ with the PES of Boothroyd, Martin, Keogh and Peterson (BMKP) [131] and $1.74 \times 10^{-13} \text{ cm}^2$ with the DJ PES [129]. For low collision energies the dynamics is sensitive to higher-order anisotropic terms in the angular expansion of the interaction potential. A diatom - diatom scattering length of 5.88 \AA was obtained for the DJ PES and 6.16 \AA for the BMKP PES. Cross sections for the quenching of rotationally excited H_2 molecules in $\text{H}_2(v=0, j=2) + \text{H}_2(v'=0, j'=0)$ and $\text{H}_2(v=0, j=2) + \text{H}_2(v'=0, j'=2)$ collisions were presented at low and ultra-low energies.

Quantum calculations of rotational relaxation of CO in cold and ultracold collisions with H_2 have recently been performed by Yang et al. [132, 133]. They reported quenching rate coefficients for $j=1-3$ of the CO molecule in collisions with both ortho- and para- H_2 [132]. Due to the relatively deep van der Waals interaction potential for the $\text{H}_2\text{-CO}$ system the

cross sections exhibit a number of narrow resonances for collision energies between $1.0 - 40.0 \text{ cm}^{-1}$. The signatures of these resonances are present in the temperature dependence of the rate coefficient which shows broad oscillatory features in the temperature range of $10^{-2} - 50 \text{ K}$ [132].

Bohn and co-workers have reported extensive calculations of hyperfine transitions in ultracold molecule - molecule collisions. Avdeenkov and Bohn studied ultracold collisions between O_2 molecules [134]. They used a quantum mechanical formalism based on the rigid rotor model and included the electronic spin structure of the O_2 molecules. Couplings between the rotational angular momentum and the electronic spin of the molecules lead to rotational fine structure. Avdeenkov and Bohn discussed the elastic and inelastic loss processes in $^{17}\text{O}_2 + ^{17}\text{O}_2$ and $^{16}\text{O}_2 + ^{16}\text{O}_2$ collisions. They found that for collision energies below 10^{-2} K , elastic collision cross sections are larger than inelastic spin-flipping transitions. Based on relative magnitudes of elastic and inelastic spin-flipping cross sections they concluded that $^{17}\text{O}_2$ molecules would be good candidates for evaporative cooling. In contrast, for $^{16}\text{O}_2 + ^{16}\text{O}_2$ collisions, inelastic processes are more efficient than elastic collisions so that $^{16}\text{O}_2$ molecules are prone to collisional trap loss.

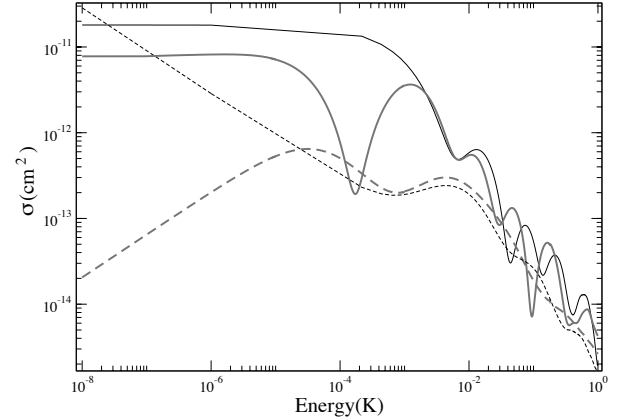


FIG. 24: Elastic and inelastic cross sections for OD + OD (thick gray line) and OH + OH (thin black line) collisions for an applied electric field of $\epsilon=100 \text{ V/cm}$. Solid and dashed lines refer to elastic and inelastic cross sections, respectively. Reproduced with permission from Avdeenkov et al. [137].

Avdeenkov and Bohn also studied ultracold collisions between OH [135, 136] and OD radicals [137] in the presence of an applied electric field. They showed that [137], elastic scattering is more efficient than inelastic processes for ultracold collisions between fermionic OD molecules, inhibiting state changing collisions. The energy dependence of elastic and inelastic cross sections for OH + OH and OD + OD collisions is illustrated in Fig. 24 for an applied electric field of $\epsilon=100 \text{ V/cm}$. While the elastic

cross sections approach finite values in the Wigner regime for the bosonic system of OH molecules and the fermionic system of OD molecules, the inelastic cross sections exhibit a totally different behavior. At ultra-low energies when molecules interact with an electric field, s-wave scattering yields an inelastic cross section diverging as $E_{coll}^{-1/2}$ for bosonic systems, while p-wave scattering yields an inelastic cross section vanishing as $E_{coll}^{1/2}$ for fermionic systems. Thus, the inelastic processes are suppressed for the fermionic system. The differences are attributed to the bosonic/fermionic character of the molecules and to the applied electric field. In the absence of an applied electric field, the elastic cross section of the fermionic system would decrease as E_{coll}^2 , faster than the inelastic cross section, which decreases as $E_{coll}^{1/2}$. Ticknor and Bohn [138] subsequently studied OH–OH collisions in the presence of a magnetic field. They showed that magnetic fields of several thousand gauss reduce inelastic collisions by about two orders of magnitude. Based on these results, they concluded that magnetic trapping may be favorable for OH molecules.

B. Vibrationally inelastic transitions

The theoretical studies presented above for molecule - molecule collisions refer to rigid rotor molecules. Pogrebnya and Clary [139, 140] have investigated vibrational relaxation in collisions of hydrogen molecules using a full-dimensional quantum dynamics formalism with an angular momentum decoupling approximation in the body fixed frame. They studied $H_2(v=1, j) + H_2(v=0, j')$ collisions involving both para-para and ortho-ortho combinations for collision energies of 1 meV (11.6 K) to 1 eV (11604 K). Time-dependent quantum mechanical calculations based on the multiconfiguration time-dependent Hartree approach have been recently applied to study full-dimensional quantum dynamics of the H_2 – H_2 system [141, 142]. These methods are suitable at high collision energies and have not been applied to cold and ultracold collisions. Very recently, vibrational energy transfer mechanism for ultracold collisions between para-hydrogen molecules has been explored by Quémener et al. [143] using a full-dimensional quantum theoretical formalism implemented in a new code written by Krems [144]. The quantum scattering calculations are based on the theory described by Arthurs and Dalgarno [145], Takayanagi [146], Green [147], and Alexander and DePristo [148]. The H_2 molecules were initially in different quantum states characterized by the vibrational quantum number v and the rotational angular momentum j . A combination of two ro-vibrational states of H_2 was referred to as a combined molecular state (CMS). A CMS, denoted as $(vjv'j')$, represents a unique quantum state of the diatom - diatom system before or after a collision.

The cross sections for $H_2(v=1, j=0) + H_2(v=$

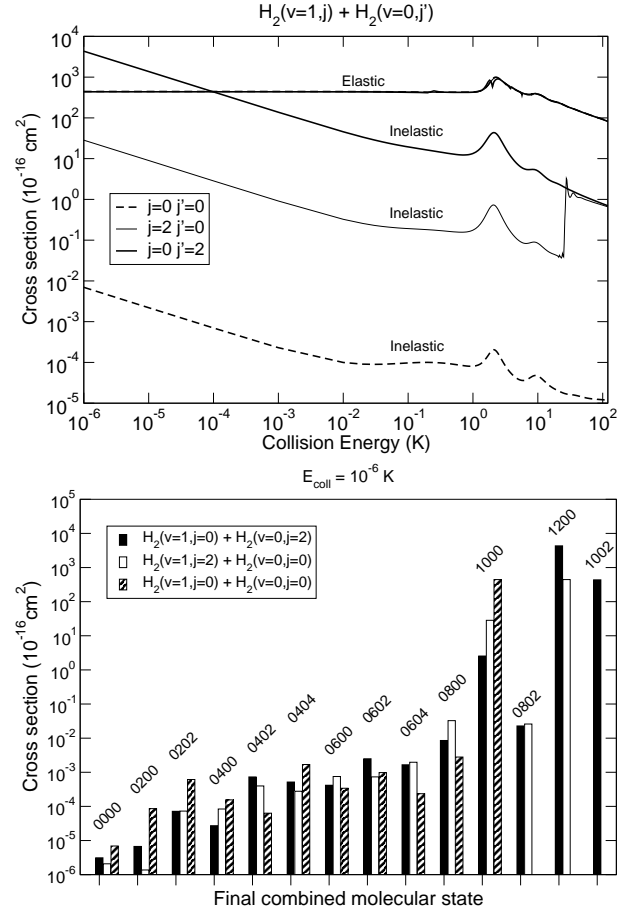


FIG. 25: Elastic and inelastic cross sections for the collisions $H_2(v=1, j=0) + H_2(v=0, j=0)$, $H_2(v=1, j=2) + H_2(v=0, j=0)$, and $H_2(v=1, j=0) + H_2(v=0, j=2)$: total cross sections (upper panel); state-to-state cross sections at 10^{-6} K (lower panel). Adapted with permission from Quémener et al. [143].

$0, j=0)$, $H_2(v=1, j=2) + H_2(v=0, j=0)$ and $H_2(v=1, j=0) + H_2(v=0, j=2)$ collisions are presented in the upper panel of Fig. 25. Using the CMS notation, this corresponds, respectively, to initial CMSs (1000), (1200) and (1002). The elastic cross sections are almost independent of the different initial ro-vibrational states of the molecules, but the inelastic cross sections are strongly dependent on the initial rotational and vibrational levels of the H_2 molecules. At 10^{-6} K , the inelastic relaxation of $H_2(v=1, j=0)$ is almost six orders of magnitude more efficient in collisions of $H_2(v=0, j=2)$ than in collisions with $H_2(v=0, j=0)$ and two orders of magnitude more efficient than in collisions of $H_2(v=1, j=2)$ with $H_2(v=0, j=0)$. At 25.45 K, which corresponds to the energy difference between the CMSs (1002) and (1200), the inelastic cross sections become comparable for $H_2(v=1, j=2) + H_2(v=0, j=0)$ and $H_2(v=1, j=0) + H_2(v=0, j=2)$ collisions. The inelastic scattering depends on the type and the combination of ro-

vibrational levels involved in the collision, whether it involves ground state molecules, $\text{H}_2(v=0, j=0)$, vibrationally excited molecules, $\text{H}_2(v=1, j=0)$, rotationally excited molecules $\text{H}_2(v=0, j=2)$, or ro-vibrationally excited molecules, $\text{H}_2(v=1, j=2)$. H_2 molecules are weakly interacting and characterized by shallow van der Waals interaction at large separations and the computed rate coefficients are not representative of strongly interacting alkali-metal dimer systems. For example, Mukaiyama et al. [109] reported an inelastic rate coefficient of $5.1 \times 10^{-11} \text{ cm}^3 \text{ s}^{-1}$ for collisions between two weakly bound Na_2 molecules created by the Feshbach resonance method. In a similar study Syassen et al. [110] reported a rate coefficient of $3 \times 10^{-10} \text{ cm}^3 \text{ s}^{-1}$ for collisions between two Rb_2 molecules. Zahzam et al. [107] estimated a rate coefficient of about $10^{-11} \text{ cm}^3 \text{ s}^{-1}$ for collisions between Cs_2 molecules. Ferlino et al. [149] measured a rate coefficient of $9 \times 10^{-11} \text{ cm}^3 \text{ s}^{-1}$ for collisions between Cs_2 molecules in the non-halo regime. The latter authors also measured the variation of the inelastic rate coefficient as a function of the atom - atom scattering length for collisions between tunable halo dimers of Cs_2 . The large values of the inelastic rate coefficients for alkali-metal dimer systems are attributed to strong inelastic couplings and deeper potential energy wells.

The state-to-state cross sections for three ro-vibrational combinations of the $\text{H}_2\text{-H}_2$ system are presented in the lower panel of Fig. 25. The magnitude of the inelastic cross sections depends on the propensity of the diatom - diatom system to conserve the internal energy and the total rotational angular momentum of the colliding molecules [143]. The final state-to-state distribution in $\text{H}_2(v=1, j=0) + \text{H}_2(v=0, j=0)$ collisions shows that there is no preferential population of rotational quantum number of either of the colliding molecules. The conservation of the total rotational angular momentum would entail a large change in the internal energy of the molecules. Thus, the purely vibrational transition $(1000) \rightarrow (0000)$ is not efficient because the energy gap is large. On the other hand, (near) conservation of the internal energy requires a large change in the total rotational angular momentum of the colliding molecules and the transition $(1000) \rightarrow (0800)$ is not dominant either. However, the state-to-state cross sections for $\text{H}_2(v=1, j=2) + \text{H}_2(v=0, j=0)$ collisions indicate that the transition $(1200) \rightarrow (1000)$ is more efficient than all the other transitions combined. For this transition, the total rotational angular momentum change and the internal energy transfer are both minimized, leading to a more efficient energy transfer process. The state-to-state cross sections for $\text{H}_2(v=1, j=0) + \text{H}_2(v=0, j=2)$ collisions present an interesting scenario in which the transition $(1002) \rightarrow (1200)$ is highly efficient and selective. In this case, the total rotational angular momentum is conserved and the internal energy is almost unchanged (the energy gap between (1200) and (1002) is only 25.45 K). This creates a favorable situation

leading to a near-resonant energy transfer process. This particular mechanism cannot occur in atom - diatom systems because simultaneous conservation of rotational angular momentum and internal energy of the molecule cannot occur. The mechanism is reminiscent of quasi-resonant energy transfer in collisions of rotationally excited diatomic molecules with atoms discussed previously [21, 53, 54, 60], but with a purely quantum origin. The near-resonant process may be an important mechanism for collisional energy transfer in ultracold molecules formed by photoassociation of ultracold atoms and for chemical reactions producing identical molecules.

Table V provides a compilation of zero-temperature rate coefficients for rotational and vibrational quenching in molecule - molecule systems.

system	initial (v, j, v', j')	$k_{T=0} (\text{cm}^3 \text{s}^{-1})$	Ref.
$\text{H}_2 + \text{H}_2$	$(v=1, j=0, v'=0, j'=0)$	8.9×10^{-18}	[143]
	$(v=2, j=0, v'=0, j'=0)$	3.9×10^{-17}	[143]
	$(v=3, j=0, v'=0, j'=0)$	1.2×10^{-16}	[143]
	$(v=4, j=0, v'=0, j'=0)$	1.8×10^{-16}	[143]
	$(v=5, j=0, v'=0, j'=0)$	6.9×10^{-16}	[143]
	$(v=6, j=0, v'=0, j'=0)$	2.9×10^{-15}	[143]
	$(v=1, j=0, v'=1, j'=0)$	2.7×10^{-16}	[143]
	$(v=2, j=0, v'=1, j'=0)$	1.3×10^{-14}	[143]
	$(v=3, j=0, v'=1, j'=0)$	1.6×10^{-14}	[143]
	$(v=4, j=0, v'=1, j'=0)$	9.0×10^{-15}	[143]
$\text{H}_2 + \text{H}_2$	$(v=2, j=0, v'=2, j'=0)$	6.1×10^{-16}	[143]
	$(v=0, j=2, v'=0, j'=0)$	3.9×10^{-14}	[143]
	$(v=1, j=2, v'=0, j'=0)$	3.7×10^{-14}	[143]
	$(v=2, j=2, v'=0, j'=0)$	8.7×10^{-14}	[143]
	$(v=3, j=2, v'=0, j'=0)$	1.5×10^{-13}	[143]
	$(v=4, j=2, v'=0, j'=0)$	2.5×10^{-13}	[143]
	$(v=1, j=2, v'=1, j'=0)$	8.8×10^{-14}	[143]
$\text{H}_2 + \text{H}_2$	$(v=2, j=2, v'=1, j'=0)$	6.1×10^{-14}	[143]
	$(v=1, j=0, v'=0, j'=2)$	5.6×10^{-12}	[143]
	$(v=2, j=0, v'=0, j'=2)$	3.4×10^{-12}	[143]
	$(v=3, j=0, v'=0, j'=2)$	2.7×10^{-12}	[143]
	$(v=4, j=0, v'=0, j'=2)$	2.1×10^{-12}	[143]
$\text{H}_2 + \text{CO}$	$(v=2, j=0, v'=1, j'=2)$	5.2×10^{-12}	[143]
	$(v=0, j=0, v'=0, j'=1)$	2.0×10^{-12}	[132]
	$(v=0, j=0, v'=0, j'=2)$	3.0×10^{-11}	[132]
$\text{H}_2 + \text{CO}$	$(v=0, j=0, v'=0, j'=3)$	1.2×10^{-10}	[132]
	$(v=0, j=1, v'=0, j'=1)$	1.2×10^{-11}	[132]
	$(v=0, j=1, v'=0, j'=2)$	4.0×10^{-11}	[132]
$\text{H}_2 + \text{CO}$	$(v=0, j=1, v'=0, j'=3)$	8.5×10^{-11}	[132]

TABLE V: Zero-temperature inelastic rate coefficients for different molecule - molecule systems.

V. SUMMARY AND OUTLOOK

In this chapter we have given an overview of recent theoretical studies of atom - molecule and molecule - molecule collisions at cold and ultracold temperatures. Though such systems have been extensively studied at higher collision energies over the last few decades, the new experimental breakthroughs in creating dense samples of cold and ultracold molecules have provided unprecedented opportunities to explore elastic, inelastic, and reactive collisions at temperatures close to absolute zero. These studies have revealed unique aspects of molecular collisions and energy transfer mechanisms that are otherwise not evident in thermal energy collisions.

The long duration of collisions combined with large de Broglie wavelengths at cold and ultracold temperatures leads to interesting quantum effects. Calculations have shown that reactions with insurmountable energy barriers may still occur at temperatures close to absolute zero, and in certain cases, with appreciable rate coefficients. Such tunneling dominated reactions have been the topic of many recent investigations and may soon be amenable to experimental investigation in the cold and ultracold regime. That the rates of these reactions can be enhanced by vibrational excitation of the molecule is an interesting scenario for experimental studies of ultracold chemical reactions.

The studies of alkali-metal homonuclear and heteronuclear trimer systems have stimulated considerable experimental interest in investigating chemical reactivity at ultracold temperatures. The challenge for theory is to describe collisions involving highly vibrationally excited molecules. Recent theoretical calculations have indicated that the three-body interaction potential can be neglected for highly vibrationally excited molecules

offering significant savings in computational effort. Even so, heavier alkali-metal trimer systems pose a daunting computational challenge.

The quantitative description of ultracold molecule - molecule collisions is another challenging topic. The recent progress on the $\text{H}_2\text{--H}_2$ system will be difficult to implement for heavier systems due to the large number of ro-vibrational levels of the molecules. The study of $\text{H}_2\text{--H}_2$ collisions has shown that, for certain combinations of ro-vibrational levels, the energy transfer may occur to specific final ro-vibrational states. In such cases, the calculations can use a much smaller basis set without compromising the accuracy.

Currently there is substantial interest in controlling the collisional outcome using external electric and magnetic fields. While the idea of coherent control of molecular collisions and chemical reactivity has existed for a long time and some important progress has been achieved, the possibility of creating coherent and dense samples of molecules in specific quantum states has given further impetus to the field of controlled chemistry. We expect that the coming years will see a far greater activity in this direction driven by cold and ultracold molecules and also by the possibility of controlling chemical reactivity using external electric and magnetic fields. Electronically non-adiabatic effects in ultracold collisions is a largely unexplored area, which can be expected to attract much attention.

Acknowledgments: This work was supported by NSF grants # PHY-0555565 (N.B.), AST-0607524 (N.B.), and by the Chemical Science, Geoscience and Bioscience Division of the Office of Basic Energy Science, Office of Science, U.S. Department of Energy (A.D.).

-
- [1] J. Doyle, B. Friedrich, R. V. Krems, and F. Masnou-Seeuws, "Editorial: Quo vadis, cold molecules?", *Eur. Phys. J. D* **31**, 149 (2004).
 - [2] R. V. Krems, "Cold controlled chemistry", *Phys. Chem. Chem. Phys.* **10**, 4079 (2008).
 - [3] J. T. Bahns, W. Stwalley, and P. L. Gould, "Formation of cold ($T \leq 1\text{K}$) molecules", *Adv. At. Mol. Opt. Phys.* **42**, 171 (2000).
 - [4] F. Masnou-Seeuws and P. Pillet, "Formation of ultracold molecules ($T < 200\ \mu\text{K}$) via photoassociation in a gas of laser-cooled atoms", *Adv. At. Mol. Opt. Phys.* **47**, 53 (2001).
 - [5] H. L. Bethlem and G. Meijer, "Production and application of translationally cold molecules", *Int. Rev. Phys. Chem.* **22**, 73 (2003).
 - [6] J. M. Hutson and P. Soldán, "Molecule formation in ultracold atomic gases", *Int. Rev. Phys. Chem.* **25**, 497 (2006).
 - [7] S. Willitsch, M. T. Bell, A. D. Gingell, S. R. Procter, and T. P. Softley, "Cold reactive collisions between laser-cooled ions and velocity-selected neutral molecules", *Phys. Rev. Lett.* **100**, 043203 (2008).
 - [8] R. V. Krems, "Molecules near absolute zero and external field control of atomic and molecular dynamics", *Int. Rev. Phys. Chem.* **24**, 99 (2005).
 - [9] E. P. Wigner, "On the behavior of cross sections near thresholds", *Phys. Rev.* **73**, 1002 (1948).
 - [10] N. Balakrishnan, V. Kharchenko, R. C. Forrey, and A. Dalgarno, "Complex scattering lengths in multi-channel atom-molecule collisions", *Chem. Phys. Lett.* **280**, 5 (1997).
 - [11] N. Balakrishnan and A. Dalgarno, "Chemistry at ultracold temperatures", *Chem. Phys. Lett.* **341**, 652 (2001).
 - [12] P. S. Zuev, R. S. Sheridan, T. V. Albu, D. G. Truhlar, D. A. Hrovat, and W. T. Borden, "Carbon tunneling from a single quantum state", *Science* **299**, 867 (2003).
 - [13] P. F. Weck and N. Balakrishnan, "Importance of long-range interactions in chemical reactions at cold and ul-

- tracold temperatures”, *Int. Rev. Phys. Chem.* **25**, 283 (2006).
- [14] J. M. Hutson and P. Soldán, “Molecular collisions in ultracold atomic gases”, *Int. Rev. Phys. Chem.* **26**, 1 (2007).
- [15] E. Bodo and F. A. Gianturco, “Collisional quenching of molecular ro-vibrational energy by He buffer loading at ultralow energies”, *Int. Rev. Phys. Chem.* **25**, 313 (2006).
- [16] T. Takayanagi, N. Masaki, K. Nakamura, M. Okamoto, and G. C. Schatz, “The rate constants for the $\text{H}+\text{H}_2$ reaction and its isotopic analogs at low temperatures: Wigner threshold law behavior”, *J. Chem. Phys.* **86**, 6133 (1987).
- [17] G. C. Hancock, C. A. Mead, D. G. Truhlar, and A. J. C. Varandas, “Reaction rates of $\text{H}(\text{H}_2)$, $\text{D}(\text{H}_2)$, and $\text{H}(\text{D}_2)$ van der Waals molecules and the threshold behavior of the bimolecular gas-phase rate coefficient”, *J. Chem. Phys.* **91**, 3492 (1989).
- [18] T. Takayanagi and S. Sato, “The bending-corrected-rotating-linear-model calculations of the rate constants for the $\text{H}+\text{H}_2$ reaction and its isotopic variants at low temperatures: The effect of van der Waals well”, *J. Chem. Phys.* **92**, 2862 (1990).
- [19] N. Balakrishnan, R. C. Forrey, and A. Dalgarno, “Quenching of H_2 vibrations in ultracold ^3He and ^4He collisions”, *Phys. Rev. Lett.* **80**, 3224 (1998).
- [20] R. C. Forrey, N. Balakrishnan, V. Kharchenko, and A. Dalgarno, “Feshbach resonances in ultracold atom-diatom scattering”, *Phys. Rev. A* **58**, R2645 (1998).
- [21] R. C. Forrey, N. Balakrishnan, A. Dalgarno, M. R. Haggerty, and E. J. Heller, “Quasiresonant energy transfer in ultracold atom-diatom collisions”, *Phys. Rev. Lett.* **82**, 2657 (1999).
- [22] R. C. Forrey, V. Kharchenko, N. Balakrishnan, and A. Dalgarno, “Vibrational relaxation of trapped molecules”, *Phys. Rev. A* **59**, 2146 (1999).
- [23] N. Balakrishnan, R. C. Forrey, and A. Dalgarno, “Vibrational relaxation of CO by collisions with ^4He at ultracold temperatures”, *J. Chem. Phys.* **113**, 621 (2000).
- [24] C. Zhu, N. Balakrishnan, and A. Dalgarno, “Vibrational relaxation of CO in ultracold ^3He collisions”, *J. Chem. Phys.* **115**, 1335 (2001).
- [25] N. Balakrishnan and A. Dalgarno, “On the quenching of rovibrationally excited molecular oxygen at ultracold temperatures”, *J. Phys. Chem. A* **105**, 2348 (2001).
- [26] P. Muchnik and A. Russek, “The HeH_2 energy surface”, *J. Chem. Phys.* **100**, 4336 (1994).
- [27] G. J. Wilson, M. L. Turnidge, A. S. Solodukhin, and C. J. S. M. Simpson, “The measurement of rate constants for the vibrational deactivation of $^{12}\text{C}^{16}\text{O}$ by H_2 , D_2 and ^4He in the gas phase down to 35 K”, *Chem. Phys. Lett.* **207**, 521 (1993).
- [28] N. Balakrishnan, R. C. Forrey, and A. Dalgarno, “Threshold phenomena in ultracold atom-molecule collisions”, *Chem. Phys. Lett.* **280**, 1 (1997).
- [29] E. I. Dashevskaya, J. A. Kunc, E. E. Nikitin, and I. Oref, “Two-channel vibrational relaxation of H_2 by He: A bridge between the Landau–Teller and Bethe–Wigner limits”, *J. Chem. Phys.* **118**, 3141 (2003).
- [30] R. Côté, E. I. Dashevskaya, E. E. Nikitin, and J. Troe, “Quantum enhancement of vibrational predissociation near the dissociation threshold”, *Phys. Rev. A* **69**, 012704 (2004).
- [31] N. Uudus, S. Magaki, and N. Balakrishnan, “Quantum mechanical investigation of ro-vibrational relaxation of H_2 and D_2 by collisions with Ar atoms”, *J. Chem. Phys.* **122**, 024304 (2005).
- [32] T.-G. Lee, C. Rochow, R. Martin, T. K. Clark, R. C. Forrey, N. Balakrishnan, P. C. Stancil, D. R. Schultz, A. Dalgarno, and G. J. Ferland, “Close-coupling calculations of low-energy inelastic and elastic processes in ^4He collisions with H_2 : A comparative study of two potential energy surfaces”, *J. Chem. Phys.* **122**, 024307 (2005).
- [33] A. I. Boothroyd, P. G. Martin, and M. R. Peterson, “Accurate analytic HeH_2 potential energy surface from a greatly expanded set of ab initio energies”, *J. Chem. Phys.* **119**, 3187 (2003).
- [34] J. P. Reid, C. J. S. M. Simpson, and H. M. Quiney, “A new HeCO interaction energy surface with vibrational coordinate dependence. II. The vibrational deactivation of $\text{CO}(v=1)$ by inelastic collisions with ^3He and ^4He ”, *J. Chem. Phys.* **107**, 9929 (1997).
- [35] R. V. Krems, “Vibrational relaxation of vibrationally and rotationally excited CO molecules by He atoms”, *J. Chem. Phys.* **116**, 4517 (2002).
- [36] R. V. Krems, “Vibrational relaxation in $\text{CO}+\text{He}$ collisions: Sensitivity to interaction potential and details of quantum calculations”, *J. Chem. Phys.* **116**, 4525 (2002).
- [37] E. Bodo, F. A. Gianturco, and A. Dalgarno, “Quenching of vibrationally excited $\text{CO}(v=2)$ molecules by ultracold collisions with ^4He atoms”, *Chem. Phys. Lett.* **353**, 127 (2002).
- [38] T. Stoecklin, A. Voronin, and J. C. Rayez, “Vibrational deactivation of $\text{F}_2(v=1, j=0)$ by ^3He at very low energy: A comparative study with the He-N_2 collision”, *Phys. Rev. A* **68**, 032716 (2003).
- [39] T. Stoecklin, A. Voronin, and J. C. Rayez, “Vibrational quenching of $\text{HF}(v=1, j)$ molecules by ^3He atoms at very low energy”, *Chem. Phys.* **294**, 117 (2003).
- [40] E. Bodo and F. A. Gianturco, “Collisional cooling of polar diatomics in ^3He and ^4He buffer gas: a quantum calculation at ultralow energies”, *J. Phys. Chem. A* **107**, 7328 (2003).
- [41] W. C. Campbell, E. Tsikata, H.-I. Lu, L. D. van Buuren, and J. M. Doyle, “Magnetic trapping and Zeeman relaxation of $\text{NH}(X^3\Sigma^-)$ ”, *Phys. Rev. Lett.* **98**, 213001 (2007).
- [42] S. Hoekstra, M. Metsälä, P. C. Zieger, L. Scharfenberg, J. J. Gilijamse, G. Meijer, and S. Y. T. van de Meerakker, “Electrostatic trapping of metastable NH molecules”, *Phys. Rev. A* **76**, 063408 (2007).
- [43] S. Y. T. van de Meerakker, P. H. M. Smeets, N. Vanhaecke, R. T. Jongma, and G. Meijer, “Deceleration and electrostatic trapping of OH radicals”, *Phys. Rev. Lett.* **94**, 023004 (2005).
- [44] B. C. Sawyer, B. L. Lev, E. R. Hudson, B. K. Stuhl, M. Lara, J. L. Bohn, and J. Ye, “Magneto-electrostatic trapping of ground state OH molecules”, *Phys. Rev. Lett.* **98**, 253002 (2007).
- [45] R. V. Krems, H. R. Sadeghpour, A. Dalgarno, D. Zgid, J. Klos, and G. Chalasinski, “Low-temperature collisions of $\text{NH}(X^3\Sigma^-)$ molecules with He atoms in a magnetic field: An ab initio study”, *Phys. Rev. A* **68**, 051401(R) (2003).
- [46] R. V. Krems, H. R. Sadeghpour, A. Dalgarno, J. Klos,

- G. C. Groenenboom, A. van der Avoird, D. Zgid, and G. Chalasinski, "Interaction of $\text{NH}(X^3\Sigma^-)$ with He: Potential energy surface, bound states, and collisional Zeeman relaxation", *J. Chem. Phys.* **122**, 094307 (2005).
- [47] L. González-Sánchez, E. Bodo, and F. A. Gianturco, "Quantum scattering of $\text{OH}(X^2\Pi)$ with $\text{He}(^1\text{S})$: Propensity features in rotational relaxation at ultralow energies", *Phys. Rev. A* **73**, 022703 (2006).
- [48] J. D. Weinstein, R. deCarvalho, T. Guillet, B. Friedrich, and J. M. Doyle, "Magnetic trapping of calcium monohydride molecules at millikelvin temperatures", *Nature* **395**, 148 (1998).
- [49] N. Balakrishnan, G. C. Groenenboom, R. V. Krems, and A. Dalgarno, "The $\text{HeCaH}(^2\Sigma^+)$ interaction. II. Collisions at cold and ultracold temperatures", *J. Chem. Phys.* **118**, 7386 (2003).
- [50] G. C. Groenenboom and N. Balakrishnan, "The $\text{HeCaH}(^2\Sigma^+)$ interaction. I. Three-dimensional ab initio potential energy surface", *J. Chem. Phys.* **118**, 7380 (2003).
- [51] R. V. Krems, A. Dalgarno, N. Balakrishnan, and G. C. Groenenboom, "Spin-flipping transitions in $^2\Sigma$ molecules induced by collisions with structureless atoms", *Phys. Rev. A* **67**, 060703(R) (2003).
- [52] R. V. Krems, "Breaking van der Waals molecules with magnetic fields", *Phys. Rev. Lett.* **93**, 013201 (2004).
- [53] B. Stewart, P. D. Magill, T. P. Scott, J. Derouard, and D. E. Pritchard, "Quasiresonant vibration-rotation transfer in atom-diatom collisions", *Phys. Rev. Lett.* **60**, 282 (1988).
- [54] P. D. Magill, B. Stewart, N. Smith, and D. E. Pritchard, "Dynamics of quasiresonant vibration-rotation transfer in atom-diatom scattering", *Phys. Rev. Lett.* **60**, 1943 (1988).
- [55] R. C. Forrey, N. Balakrishnan, A. Dalgarno, M. R. Haggerty, and E. J. Heller, "The effect of quasiresonant dynamics on the predissociation of van der Waals molecules", *Phys. Rev. A* **64**, 022706 (2001).
- [56] R. C. Forrey, "Prospects for cooling and trapping rotationally hot molecules", *Phys. Rev. A* **66**, 023411 (2002).
- [57] J. C. Flasher and R. C. Forrey, "Cold collisions between argon atoms and hydrogen molecules", *Phys. Rev. A* **65**, 032710 (2002).
- [58] P. Florian, M. Hoster, and R. C. Forrey, "Rotational relaxation in ultracold $\text{CO}+\text{He}$ collisions", *Phys. Rev. A* **70**, 032709 (2004).
- [59] A. Mack, T. K. Clark, R. C. Forrey, N. Balakrishnan, T.-G. Lee, and P. C. Stancil, "Cold $\text{He}+\text{H}_2$ collisions near dissociation", *Phys. Rev. A* **74**, 052718 (2006).
- [60] A. Ruiz and E. J. Heller, "Quasiresonance", *Mol. Phys.* **104**, 127 (2006).
- [61] A. J. McCaffery, "Vibration-rotation transfer in molecular super rotors", *J. Chem. Phys.* **113**, 10947 (2000).
- [62] A. J. McCaffery and R. J. Marsh, "Vibrational predissociation of van der Waals molecules: An internal collision, angular momentum model", *J. Chem. Phys.* **117**, 9275 (2002).
- [63] R. J. Marsh and A. J. McCaffery, "Quantitative prediction of collision-induced vibration-rotation distributions from physical data", *J. Phys. B: At. Mol. Opt. Phys.* **36**, 1363 (2003).
- [64] E. Bodo, E. Scifoni, F. Sebastianelli, F. A. Gianturco, and A. Dalgarno, "Rotational quenching in ionic systems at ultracold temperatures", *Phys. Rev. Lett.* **89**, 283201 (2002).
- [65] T. Stoecklin and A. Voronin, "Strong isotope effect in ultracold collision of $\text{N}_2^+(\nu=1, j=0)$ with He: A case study of virtual-state scattering", *Phys. Rev. A* **72**, 042714 (2005).
- [66] G. Guillon, T. Stoecklin and A. Voronin, "Spin-rotation interaction in cold and ultracold collisions of $\text{N}_2^+(^2\Sigma^+)$ with ^3He and ^4He ", *Phys. Rev. A* **75**, 052722 (2007).
- [67] S. C. Althorpe and D. C. Clary, "Quantum scattering calculations on chemical reactions", *Annu. Rev. Phys. Chem.* **54**, 493 (2003).
- [68] W. Hu and G. C. Schatz, "Theories of reactive scattering", *J. Chem. Phys.* **125**, 132301 (2006).
- [69] I. W. M. Smith, "Laboratory Studies of Atmospheric Reactions at Low Temperatures", *Chem. Rev.* **103**, 4549 (2003).
- [70] J. F. Castillo, D. E. Manolopoulos, K. Stark, and H.-J. Werner, "Quantum mechanical angular distributions for the $\text{F}+\text{H}_2$ reaction", *J. Chem. Phys.* **104**, 6531 (1996).
- [71] T. Takayanagi and Y. Kurosaki, "van der Waals resonances in cumulative reaction probabilities for the $\text{F}+\text{H}_2$, D_2 , and HD reactions", *J. Chem. Phys.* **109**, 8929 (1998).
- [72] R. T. Skodje, D. Skouteris, D. E. Manolopoulos, S.-H. Lee, F. Dong, and K. Liu, "Resonance-mediated chemical reaction: $\text{F}+\text{HD} \rightarrow \text{HF}+\text{D}$ ", *Phys. Rev. Lett.* **85**, 1206 (2000).
- [73] E. Bodo, F. A. Gianturco, and A. Dalgarno, " $\text{F}+\text{D}_2$ reaction at ultracold temperatures", *J. Chem. Phys.* **116**, 9222 (2002).
- [74] N. Balakrishnan and A. Dalgarno, "On the isotope effect in $\text{F}+\text{HD}$ reaction at ultracold temperatures", *J. Phys. Chem. A* **107**, 7101 (2003).
- [75] E. Bodo, F. A. Gianturco, N. Balakrishnan, and A. Dalgarno, "Chemical reactions in the limit of zero kinetic energy: virtual states and Ramsauer minima in $\text{F}+\text{H}_2 \rightarrow \text{HF}+\text{H}$ ", *J. Phys. B: At. Mol. Opt. Phys.* **37**, 3641 (2004).
- [76] M. Qui, Z. Ren, L. Che, D. Dai, A. A. Harich, X. Wang, X. Yang, C. Xu, D. Xie, M. Gustafsson, R. T. Skodje, Z. Sun, and D. H. Zhang, "Observation of Feshbach resonances in the $\text{F}+\text{H}_2 \rightarrow \text{HF}+\text{H}$ reaction", *Science* **311**, 1440 (2006).
- [77] J. Aldegunde, J. M. Alvarino, M. P. de Miranda, V. Sáez Rábanos, and F. J. Aoiz, "Mechanism and control of the $\text{F}+\text{H}_2$ reaction at low and ultralow collision energies", *J. Chem. Phys.* **125**, 133104 (2006).
- [78] S.-H. Lee, F. Dong, and K. Liu, "A crossed-beam study of the $\text{F}+\text{HD} \rightarrow \text{HF}+\text{D}$ reaction: The resonance-mediated channel", *J. Chem. Phys.* **125**, 133106 (2006).
- [79] L. Tao and M. H. Alexander, "Role of van der Waals resonances in the vibrational relaxation of HF by collisions with H atoms", *J. Chem. Phys.* **127**, 114301 (2007).
- [80] D. De Fazio, S. Cavalli, V. Aquilanti, A. A. Buchachenko, and T. V. Tscherbul, "On the role of scattering resonances in the $\text{F}+\text{HD}$ reaction dynamics", *J. Phys. Chem. A* **111**, 12538 (2007).
- [81] D. Skouteris, D. E. Manolopoulos, W. S. Bian, H.-J. Werner, L. H. Lai, and K. Liu, "van der Waals interactions in the $\text{Cl}+\text{HD}$ reaction", *Science* **286**, 1713 (1999).
- [82] N. Balakrishnan, "On the role of van der Waals interaction in chemical reactions at low temperatures", *J.*

- Chem. Phys. **121**, 5563 (2004).
- [83] P. F. Weck and N. Balakrishnan, “Chemical reactivity of ultracold polar molecules: investigation of $\text{H} + \text{HCl}$ and $\text{H} + \text{DCl}$ collisions”, *Eur. Phys. J. D* **31**, 417 (2004).
- [84] P. F. Weck and N. Balakrishnan, “Quantum dynamics of the $\text{Li} + \text{HF} \rightarrow \text{H} + \text{LiF}$ reaction at ultralow temperatures”, *J. Chem. Phys.* **122**, 154309 (2005).
- [85] P. F. Weck and N. Balakrishnan, “Heavy atom tunneling in chemical reactions: Study of $\text{H} + \text{LiF}$ collisions”, *J. Chem. Phys.* **122**, 234310 (2005).
- [86] P. F. Weck and N. Balakrishnan, “Reactivity enhancement of ultracold $\text{O}(^3P) + \text{H}_2$ collisions by van der Waals interactions”, *J. Chem. Phys.* **123**, 144308 (2005).
- [87] P. F. Weck, N. Balakrishnan, J. Brandao, C. Rosa, and W. Wang, “Dynamics of the $\text{O}(^3P) + \text{H}_2$ reaction at low temperatures: Comparison of quasiclassical trajectory with quantum scattering calculations”, *J. Chem. Phys.* **124**, 074308 (2006).
- [88] G. Quémener and N. Balakrishnan, “Cold and ultracold chemical reactions of $\text{F} + \text{HCl}$ and $\text{F} + \text{DCl}$ ”, *J. Chem. Phys.* **128**, 224304 (2008).
- [89] K. Stark and H.-J. Werner, “An accurate multireference configuration interaction calculation of the potential energy surface for the $\text{F} + \text{H}_2 \rightarrow \text{HF} + \text{H}$ reaction”, *J. Chem. Phys.* **104**, 6515 (1996).
- [90] M. Baer, “Strong isotope effects in the $\text{F} + \text{HD}$ reactions at the low-energy interval: a quantum-mechanical study”, *Chem. Phys. Lett.* **312**, 203 (1999).
- [91] D. H. Zhang, S.-Y. Lee, and M. Baer, “Quantum mechanical integral cross sections and rate constants for the $\text{F} + \text{HD}$ reactions”, *J. Chem. Phys.* **112**, 9802 (2000).
- [92] A. Aguado, M. Paniagua, C. Sanz, and O. Roncero, “Transition state spectroscopy of the excited electronic states of LiHF ”, *J. Chem. Phys.* **119**, 10088 (2003).
- [93] T. V. Tscherbul and R. V. Krems, “Quantum theory of chemical reactions in the presence of electromagnetic fields”, *J. Chem. Phys.* **129**, 034112 (2008).
- [94] M. T. Cvitaš, P. Soldán, J. M. Hutson, P. Honvault, and J.-M. Launay, “Ultracold $\text{Li} + \text{Li}_2$ collisions: Bosonic and fermionic cases”, *Phys. Rev. Lett.* **94**, 033201 (2005).
- [95] M. T. Cvitaš, P. Soldán, J. M. Hutson, P. Honvault, and J.-M. Launay, “Ultracold collisions involving heteronuclear alkali metal dimers”, *Phys. Rev. Lett.* **94**, 200402 (2005).
- [96] G. Quémener, J.-M. Launay, and P. Honvault, “Ultracold collisions between Li atoms and Li_2 diatoms in high vibrational states”, *Phys. Rev. A* **75**, 050701(R) (2007).
- [97] M. T. Cvitaš, P. Soldán, J. M. Hutson, P. Honvault, and J.-M. Launay, “Interactions and dynamics in $\text{Li} + \text{Li}_2$ ultracold collisions”, *J. Chem. Phys.* **127**, 074302 (2007).
- [98] P. Soldán, M. T. Cvitaš, J. M. Hutson, P. Honvault, and J.-M. Launay, “Quantum dynamics of ultracold $\text{Na} + \text{Na}_2$ collisions”, *Phys. Rev. Lett.* **89**, 153201 (2002).
- [99] G. Quémener, P. Honvault, and J.-M. Launay, “Sensitivity of the dynamics of $\text{Na} + \text{Na}_2$ collisions on the three-body interaction at ultralow energies”, *Eur. Phys. J. D* **30**, 201 (2004).
- [100] G. Quémener, P. Honvault, J.-M. Launay, P. Soldán, D. E. Potter, and J. M. Hutson, “Ultracold quantum dynamics: Spin-polarized $\text{K} + \text{K}_2$ collisions with three identical bosons or fermions”, *Phys. Rev. A* **71**, 032722 (2005).
- [101] J.-M. Launay and M. Le Dourneuf, “Hyperspherical close-coupling calculation of integral cross sections for the reaction $\text{H} + \text{H}_2 \rightarrow \text{H}_2 + \text{H}$ ”, *Chem. Phys. Lett.* **163**, 178 (1989).
- [102] J. Higgins, T. Hollebeek, J. Reho, T.-S. Ho, K. K. Lehmann, H. Rabitz, and G. Scoles, “On the importance of exchange effects in three-body interactions: The lowest quartet state of Na_3 ”, *J. Chem. Phys.* **112**, 5751 (2000).
- [103] F. D. Colavecchia, J. P. Burke, Jr., W. J. Stevens, M. R. Salazar, G. A. Parker, and R. T. Pack, “The potential energy surface for spin-aligned $\text{Li}_3(1^4A')$ and the potential energy curve for spin-aligned $\text{Li}_2(a^3\Sigma_u^+)$ ”, *J. Chem. Phys.* **118**, 5484 (2003).
- [104] D. A. Brue and G. A. Parker, “Conical intersection between the lowest spin-aligned $\text{Li}_3(1^4A')$ potential-energy surfaces”, *J. Chem. Phys.* **123**, 091101 (2005).
- [105] P. Soldán, M. T. Cvitaš, and J. M. Hutson, “Three-body nonadditive forces between spin-polarized alkali-metal atoms”, *Phys. Rev. A* **67**, 054702 (2003).
- [106] P. Staunum, S. D. Kraft, J. Lange, R. Wester, and M. Weidemüller, “Experimental investigation of ultracold atom-molecule collisions”, *Phys. Rev. Lett.* **96**, 023201 (2006).
- [107] N. Zahzam, T. Vogt, M. Mudrich, D. Comparat and P. Pillet, “Atom-molecule collisions in an optically trapped gas”, *Phys. Rev. Lett.* **96**, 023202 (2006).
- [108] R. Wynar, R. S. Freeland, D. J. Han, C. Ryu and D. J. Heinzen, “Molecules in a Bose-Einstein condensate”, *Science* **287**, 1016 (2000).
- [109] T. Mukaiyama, J. R. Abo-Shaeer, K. Xu, J. K. Chin, and W. Ketterle, “Dissociation and decay of ultracold sodium molecules”, *Phys. Rev. Lett.* **92**, 180402 (2004).
- [110] N. Syassen, T. Volz, S. Teichmann, S. Dürr, and G. Rempe, “Collisional decay of ^{87}Rb Feshbach molecules at 1005.8 G”, *Phys. Rev. A* **74**, 062706 (2006).
- [111] E. R. Hudson, N. B. Gilfoy, S. Kotochigova, J. M. Sage, and D. DeMille, “Inelastic collisions of ultracold heteronuclear molecules in an optical trap”, *Phys. Rev. Lett.* **100**, 203201 (2008).
- [112] C. Amiot and O. Dulieu, “The Cs_2 ground electronic state by Fourier transform spectroscopy: dispersion coefficients”, *J. Chem. Phys.* **117**, 5155 (2002).
- [113] A. Derevianko, W. R. Johnson, M. S. Safronova, and J. F. Babb, “High-precision calculations of dispersion coefficients, static dipole polarizabilities, and atom-wall interaction constants for alkali-metal atoms”, *Phys. Rev. Lett.* **82**, 3589 (1999).
- [114] J. M. Hutson, “Feshbach resonances in ultracold atomic and molecular collisions: threshold behaviour and suppression of poles in scattering lengths”, *New J. Phys.* **9**, 152, (2007).
- [115] W. C. Stwalley, “Collisions and reactions of ultracold molecules”, *Can. J. Chem.* **82**, 709 (2004).
- [116] D. S. Petrov, C. Salomon, and G. V. Shlyapnikov, “Weakly bound dimers of fermionic atoms”, *Phys. Rev. Lett.* **93**, 090404 (2004).
- [117] E. Bodo, F. A. Gianturco, and E. Yurtsever, “Vibrational quenching at ultralow energies: Calculations of the $\text{Li}_2(1^1\Sigma_g^+; \nu \gg 0) + \text{He}$ superelastic scattering cross sections”, *Phys. Rev. A* **73**, 052715 (2006).
- [118] A. J. Kerman, J. M. Sage, S. Sainis, T. Bergeman, and D. DeMille, “Production and state-selective detection of ultracold RbCs molecules”, *Phys. Rev. Lett.* **92**, 153001 (2004).

- (2004).
- [119] J. M. Sage, S. Sainis, T. Bergeman, and D. DeMille, “Optical production of ultracold polar molecules”, *Phys. Rev. Lett.* **94**, 203001 (2005).
 - [120] C. Haimberger, J. Kleinert, M. Bhattacharya, and N. P. Bigelow, “Formation and detection of ultracold ground-state polar molecules”, *Phys. Rev. A* **70**, 021402 (2004).
 - [121] J. Kleinert, C. Haimberger, P. J. Zabawa, and N. P. Bigelow, “Trapping of ultracold polar molecules with a thin-wire electrostatic trap”, *Phys. Rev. Lett.* **99**, 143002 (2007).
 - [122] M. W. Mancini, G. D. Telles, A. R. L. Caires, V. S. Bagnato, and L. G. Marcassa, “Observation of ultracold ground-state heteronuclear molecules”, *Phys. Rev. Lett.* **92**, 133203 (2004).
 - [123] D. Wang, J. Qi, M. F. Stone, O. Nikolayeva, B. Hattaway, S. D. Gensemer, H. Wang, W. T. Zemke, P. L. Gould, E. E. Eyler and W. C. Stwalley, “The photoassociative spectroscopy, photoassociative molecule formation, and trapping of ultracold $^{39}\text{K}^{85}\text{Rb}$ ”, *Eur. Phys. J. D* **31**, 165 (2004).
 - [124] S. D. Kraft, P. Staunum, J. Lange, L. Vogel, R. Wester, and M. Weidemüller, “Formation of ultracold LiCs molecules”, *J. Phys. B: At. Mol. Opt. Phys.* **39**, S993 (2006).
 - [125] U. Schlöder, C. Silber, and C. Zimmermann, “Photoassociation of heteronuclear lithium”, *Appl. Phys. B: Lasers Opt.* **73**, 801 (2001).
 - [126] T.-G. Lee, N. Balakrishnan, R. C. Forrey, P. C. Stancil, D. R. Schultz, and G. J. Ferland, “State-to-state rotational transitions in H_2+H_2 collisions at low temperatures”, *J. Chem. Phys.* **125**, 114302 (2006).
 - [127] R. C. Forrey, “Cooling and trapping of molecules in highly excited rotational states”, *Phys. Rev. A* **63**, 051403(R) (2001).
 - [128] B. Maté, F. Thibault, G. Tejeda, J. M. Fernández, and S. Montero, “Inelastic collisions in para- H_2 : Translation-rotation state-to-state rate coefficients and cross sections at low temperature and energy”, *J. Chem. Phys.* **122**, 064313 (2005).
 - [129] P. Diep and J. K. Johnson, “An accurate $\text{H}_2\text{-H}_2$ interaction potential from first principles”, *J. Chem. Phys.* **112**, 4465 (2000).
 - [130] S. Montero, F. Thibault, G. Tejeda, and J. M. Fernández, “Rotranslational state-to-state rates and spectral representation of inelastic collisions in low-temperature molecular hydrogen”, *J. Chem. Phys.* **125**, 124301 (2006).
 - [131] A. I. Boothroyd, P. G. Martin, W. J. Keogh, and M. J. Peterson, “An accurate analytic H_4 potential energy surface”, *J. Chem. Phys.* **116**, 666 (2002).
 - [132] B. Yang, P. C. Stancil, N. Balakrishnan, and R. C. Forrey, “Quenching of rotationally excited CO by collisions with H_2 ”, *J. Chem. Phys.* **124**, 104304 (2006).
 - [133] B. Yang, H. Perera, N. Balakrishnan, R. C. Forrey, and P. C. Stancil, “Quenching of rotationally excited CO in cold and ultracold collisions with H, He and H_2 ”, *J. Phys. B: At. Mol. Opt. Phys.* **39**, S1229 (2006).
 - [134] A. V. Avdeenkov and J. L. Bohn, “Ultracold collisions of oxygen molecules”, *Phys. Rev. A* **64**, 052703 (2001).
 - [135] A. V. Avdeenkov and J. L. Bohn, “Collisional dynamics of ultracold OH molecules in an electrostatic field”, *Phys. Rev. A* **66**, 052718 (2002).
 - [136] A. V. Avdeenkov and J. L. Bohn, “Linking Ultracold Polar Molecules”, *Phys. Rev. Lett.* **90**, 043006 (2003).
 - [137] A. V. Avdeenkov and J. L. Bohn, “Ultracold collisions of fermionic OD radicals”, *Phys. Rev. A* **71**, 022706 (2005).
 - [138] C. Ticknor and J. L. Bohn, “Influence of magnetic fields on cold collisions of polar molecules”, *Phys. Rev. A* **71**, 022709 (2005).
 - [139] S. K. Pogrebnya and D. C. Clary, “A full-dimensional quantum dynamical study of vibrational relaxation in H_2+H_2 ”, *Chem. Phys. Lett.* **363**, 523 (2002).
 - [140] S. K. Pogrebnya, M. E. Mandy and D. C. Clary, “Vibrational relaxation in H_2+H_2 : full-dimensional quantum dynamical study”, *Int. J. Mass. Spectrom.* **223-224**, 335 (2003).
 - [141] A. N. Panda, F. Otto, F. Gatti, and H.-D. Meyer, “Rovibrational energy transfer in ortho- H_2 +para- H_2 collisions”, *J. Chem. Phys.* **127**, 114310 (2007).
 - [142] F. Otto, F. Gatti, and H.-D. Meyer, “Rotational excitations in para- H_2 +para- H_2 collisions: Full- and reduced-dimensional quantum wave packet studies comparing different potential energy surfaces”, *J. Chem. Phys.* **128**, 064305 (2008).
 - [143] G. Quémener, N. Balakrishnan, and R. V. Krems, “Vibrational energy transfer in ultracold molecule-molecule collisions”, *Phys. Rev. A* **77**, 030704(R) (2008).
 - [144] R. V. Krems, TwoBC - quantum scattering program, University of British Columbia, Vancouver, Canada (2006).
 - [145] A. M. Arthurs and A. Dalgarno, “The theory of scattering by a rigid rotator”, *Proc. Roy. Soc. A* **256**, 540 (1960).
 - [146] K. Takayanagi, “The production of rotational and vibrational transitions in encounters between molecules”, *Adv. At. Mol. Phys.* **1**, 149 (1965).
 - [147] S. Green, “Rotational excitation in $\text{H}_2\text{-H}_2$ collisions: Close-coupling calculations”, *J. Chem. Phys.* **62**, 2271 (1975).
 - [148] M. H. Alexander and A. E. DePristo, “Symmetry considerations in the quantum treatment of collisions between two diatomic molecules”, *J. Chem. Phys.* **66**, 2166 (1977).
 - [149] F. Ferlaino, S. Knoop, M. Mark, M. Berninger, H. Schöbel, H.-C. Nägerl, and R. Grimm, “Collisions between tunable halo dimers: exploring an elementary four-body process with identical bosons”, *Phys. Rev. Lett.* **101**, 023201 (2008).